การสังเคราะห์แมกนีไทต์ดิสเพอร์ชันที่เคลือบด้วยแอมฟีฟิลิกพอลิเมอร์ชนิดใหม่

นายองอาจ ธเนศนิตย์

วิทยานิพนธ์นี้เป็นส่วนหนึ่งของการศึกษาตามหลักสูตรปริญญาวิทยาศาสตรดุษฎีบัณฑิต
สาขาวิชาเคมี ภาควิชาเคมี
คณะวิทยาศาสตร์ จุฬาลงกรณ์มหาวิทยาลัย
ปีการศึกษา 2552

SYNTHESIS OF NOVEL AMPHIPHILIC POLYMER-COATED MAGNETITE DISPERSION

Mr. Ong-art Thanetnit

A Dissertation Submitted in Partial Fulfillment of the Requirements
for the Degree of Doctor of Philosophy Program in Chemistry
Department of Chemistry
Faculty of Science
Chulalongkorn University
Academic Year 2009

Thesis Title	SYNTHESIS OF NOVEL AMPHIPHILIC POLYMER-COATED MAGNETITE DISPERSION
By	Mr Ong-art Thanetnit
Field of Study	Chemistry
Thesis Advisor	Associate Professor Supawan Tantayanon, Ph.D.
Thesis Co-Advisor	Associate Professor William W. Yu, Ph.D.

Accepted by the Faculty of Science, Chulalongkorn University in Partial Fulfillment of the Requirements for the Doctoral's Degree

…… Dean of the Faculty of Science
(Professor Supot Hannongbua, Dr. rer. nat.)

THESIS COMMITTEE

…….. Chairman
(Asssistant Professor Warinthorn Chavasiri, Ph.D.)

……..……. Thesis Advisor
(Associate Professor Supawan Tantayanon, Ph.D.)

……..……. Thesis Co-Advisor
(Associate Professor William W. Yu, Ph.D.)

…….. Examiner
(Associate Professor Thawatchai Tuntulani, Ph.D.)

…….. Examiner
(Associate Professor Nuanphun Chantarasiri, Ph.D.)

…….. External Examiner
(Kritapas Laohhasurayotin, Ph.D.)

องอาจ ธเนศนิตย์: การสังเคราะห์แมกนีไทต์ดิสเพอร์ชันที่เคลือบด้วยแอมฟิฟิลิกพอลิเมอร์ชนิดใหม่ (SYNTHESIS OF NOVEL AMPHIPHILIC POLYMER-COATED MAGNETITE DISPERSION) อ.ที่ปรึกษาวิทยานิพนธ์หลัก: รศ. ดร. ศุภวรรณ ตันตยานนท์, อ. ที่ปรึกษาวิทยานิพนธ์ร่วม : Associate Professor William W. Yu; 80 หน้า.

พอลิเอ็นทูไฮดรอกซิเอทิลมาลิอิมายด์โควันออกทะเดซีน และพอลิมาเลอิกแอนไฮดรายด์โควันออกทาเดซีน(พีเอ็มเอโอ) ถูกสังเคราะห์โดยรีเวอร์ซิเบิลแอดดิชันแฟลกเมนเทชันเชนทรานส-เฟอร์(แรฟต์)พอลิเมอไรเซชัน โดยใช้เอสวันโดเดซิลเอสพรายม์แอลฟาแอลฟาพรายม์ไดเมทิลแอลฟาดับเบิลพรายม์แอซีทิกแอซิดไทรไทโอคาร์บอเนต และเอสวันโดเดซิลเอสพรายม์แอลฟาแอลฟาพรายม์ไดเมทิลแอลฟาดับเบิลพรายม์เมทิลแอซีเทตไทรไทโอคาร์บอเนต เป็นสารถ่ายโอนแรฟต์ตามลำดับ พีเอ็มเอโอถูกดัดแปรที่หน่วยมาเลอิกแอนไฮดรายด์โดยการเปิดวงตามด้วยปฏิกิริยาคัปลิงของคาร์บอซิลิกที่เกิดขึ้น กับทูทูแอมิโนเอทอกซีเอทานอล เพื่อได้อนุพันธ์ของพีเอ็มเอโอ อนุภาคนาโนแมกนีไทต์โมโนดิสเพิร์สที่มีขนาดอนุภาคต่างๆ 11-32 นาโนเมตร ถูกเตรียมโดยการสลายด้วยความร้อนของไอร์ออน(III)ไฮดรอกไซด์ออกไซด์ ที่มีความเข้มข้นของโอลิอิกแอซิดต่างๆ การเกิดแมกนีไทต์คอมเพล็กซ์ทำได้โดยการผสมสารละลายพอลิเมอร์และสารละลายแมกนีไทต์โมโนดิสเพิร์สขนาด 11 นาโนเมตร ตามด้วยการเติมน้ำและการนำเอาตัวทำละลายอินทรีย์ออกจากของผสม ขณะที่แมกนีไทต์คอมเพล็กซ์ที่เตรียมได้จากอนุพันธ์พีเอ็มเอโอพบว่าเป็นสารละลายใส แต่พบตะกอนเกิดขึ้นในกรณีที่ใช้พอลิเอ็นทูไฮดรอกซิเอทิลมาลิอิมายด์โควันออกทะเดซีน นอกจากนี้สารละลายชนิดแรกเป็นดิสเพิร์สของอนุภาคนาโนที่มีขนาดเฉลี่ย 13 นาโนเมตรซึ่งแสดงให้เห็นด้วยทีอีเอ็ม ผลงานเหล่านี้บ่งชี้ว่าสามารถสังเคราะห์แมกนีไทต์ดิสเพอร์ชันที่เคลือบด้วยแอมฟิฟิลิกพอลิเมอร์ชนิดใหม่ได้สำเร็จ โคพอลิเมอร์ทั้งหมดถูกพิสูจน์เอกลักษณ์โดย เอทีอาร์ไออาร์ โปรตอนเอ็นเอ็มอาร์ คาร์บอนสิบสามเอ็นเอ็มอาร์ จีพีซี และทีจีเอ

ภาควิชา……เคมี……ลายมือชื่อนิสิต……...

สาขาวิชา……เคมี……..……..ลายมือชื่ออ.ที่ปรึกษาวิทยานิพนธ์หลัก…….…..

ปีการศึกษา……2552……ลายมือชื่ออ.ที่ปรึกษาวิทยานิพนธ์ร่วม……

4873866023 : MAJOR CHEMISTRY
KEY WORDS : AMPHIPHILIC POLYMER, MAGNETITE, NANOPARTICLES

ONG-ART : SYNTHESIS OF NOVEL AMPHIPHILIC POLYMER-COATED MAGNETITE DISPERSION. THESIS ADVISOR : ASSOC. PROF. SUPAWAN TANTAYANON, Ph. D., THESIS CO-ADVISOR : ASSOC. PROF. WILLIAM W. YU, Ph. D., 80 pp.

Poly (N-(2-hydroxyethyl)maleimide-*co*-1-octadecene) and poly(maleic anhydride-*co*-1-octadecene) (PMAO) were synthesized by reversible addition-fragmentation chain transfer (RAFT) polymerization using S-1-dodecyl-S′-(*α,α′*-dimethyl-*α″*-acetic acid) trithiocarbonate and S-1-dodecyl-S′-(*α,α′*-dimethyl-*α″*-methyl acetate) trithiocarbonate as RAFT transfer agents, respectively. PMAO was further modified at maleic anhydride moiety *via* ring opening followed by coupling reaction of the generated carboxylic acid with 2-(2-aminoethoxy)ethanol, to obtain the PMAO derivative. Monodispersed magnetite nanoparticles with different particle sizes, 11-32 nm, were prepared by thermal decomposition of iron(III) hydroxide oxide with various the oleic acid concentration. The formation of magnetite complex dispersion was generated by mixing the polymer solution and the 11 nm monodispersed magnetite solution, followed by adding water, and removing the organic solvent from the mixture. Whereas the resulting magnetite complex using PMAO derivative appeared as a clear solution, the precipitation was observed in case of using poly (N-(2-hydroxyethyl)maleimide-*co*-1-octadecene). In addition, the first solution was found to be the dispersion of nanoparticles with the average size of 13 nm as revealed by TEM. These results indicated that a novel amphiphilic polymer-coated magnetite dispersion was successfully synthesized. All copolymers were characterized by ATR-IR, ^{1}H-NMR, ^{13}C-NMR, GPC and TGA.

Department …...……Chemistry…… Student's Signature……
Field of Study ……Chemistry…… Advisor's Signature……
Academic Year …….2009…… Co-Advisor's Signature……..…….....

ACKNOWLEDGEMENTS

The author would like to express his deeply grateful acknowledgement to his advisor, Associate Professor Dr. Supawan Tantayanon, for her kind supporting, helpful guidance, understanding, valuable suggestions, supervision and continuous encouragement throughout the course of this research. The author also would like to express the grateful appreciation to his co-advisor, Associate Professor Dr. William W. Yu, for his inspiration, valuable advice, encouragement and assistance throughout the course of this research. In addition, the author wishes to express his appreciation to Prof. Jame W. Pavlik, Prof. John C. MacDonalds from Worcester Polytechnics Institute for their suggestion and assistance. The autor also would like to thank to Xinbi Li for his kind assistance and valuable discussion, especially in magnetite nanoparticles. The author would like to express his appreciated to Assistant Prof. Dr. Warinthorn Chavasiri, Associate Prof. Dr. Nuanphun Chantarasiri, Associate Prof. Dr. Thawatchai Tuntulani and Dr. Kritapas Laohhasurayotin for their comments, corrections and assistance as thesis committees.

. Moreover, thanks are extended to the graduate school for research grant, the Department of Chemistry, Faculty of Science, Chulalongkorn University and Chemistry and Biochemistry program, Worcester Polytechnics Institute for their financial supporting scholarship. The author thanks Green Chemistry Research Laboratory, Faculty of Science, Chulalongkorn University and nano-laboratory, Worcester Polytechnics Institute, for the support of chemicals and laboratory facilities.

Appreciation is also extended to all of my friends at Chulalongkorn University and Worcester Polytechnics Institute for their truly assistant, understanding and encouragement.

Special thanks are expressed to my truly family for their love, affection, best wishes, understanding and encouragement, without them, the author would have never been able to be successful on this goal.

CONTENTS

Page

Page

Page

LIST OF TABLES

LIST OF FIGURES

Page

Page

LIST OF SCHEMES

LIST OF ABBREVIATION

Au	gold
^{o}C	degree Celsius
cm^{-1}	wave number
Cu^{2+}	cuprous ion
CuBr	copper bromide
DMMAT	S-1-Dodecyl-S′-(*α,α′*-dimethyl-*α″*-acetic acid)-trithiocarbonate
DMMAAT	S-1-Dodecyl-S′-(*α,α′*-dimethyl-*α″*-methyl acetate)-trithiocarbonate
FeO(OH)	ferric oxyhydroxide
g	gram
GPC	gel permeation chromatography
h	hour
M	molarity
M_n	number averages molecular weight
M_w	weight averages molecular weight
µm	micrometer
mg	milligram
mL	milliliter
mL/ min	millilitre per minute
min	minute
mol L^{-1}	mol per liter
nm	nanometre
PDI	polydispersity index
PMAO	poly(maleic anhydride-*co*-1-octadecene)
RAFT	radical addition–fragmentation transfer
TEM	transmission electron microscopy
THF	tetrahydrofuran

CHAPTER I

INTRODUCTION

1.1 Introduction

Magnetic particles have been attracted much interest in recent years because of their unique properties such as superparamagnetism [1]. They are widely used in many technological applications such as catalysis [2], magnetic recording [3], high performance electromagnetic [4] and spintronic devices [5], as well as environmental remediation [6] and biomedical applications, such as magnetic resonance imaging (MRI) [7], cell and protein separation [8], and drug delivery [9].

Magnetite (Fe_3O_4) nanoparticles are acclaimed as one of the excellent candidates for the size dependent magnetic materials. It is well known that magnetite nanoparticles is numerously used in many applications, especially biomedical applications, such as MRI contrast enhancement, tissue repair, immunoassay, detoxification of biological fluids, hyperthermia, drug delivery, and cell separation [10]. There are numerous chemical methods to synthesize magnetite nanoparticles such as chemical co-precipitation of iron salt [11], microemulsion [12], sol-gel synthesis [13], sonochemical [14], and hydrolysis and thermolysis of precursor [15]. As the matter of fact, magnetite is extremely unstable and is sensitive to oxidation in air and could be turned into maghemite. To prevent these obstacles, most synthetic methods are required to modify surface of magnetite or coat nanoparticles with organic materials, such as biomaterials and polymers, to produce an electrostatic or steric repulsive force [16-17].

In recent years, the field of living free-radical polymerization has been revolutionized by the development of techniques for controlling the molecular weight and the architecture of polymer chains. Among the most versatile approaches, the

reversible addition-fragmentation chain transfer (RAFT) polymerization is carried out with chain transfer agents, such as thiocarbonylthio compounds, which reversibly react with growing radicals via chain transfer reactions [18]. Consequently, chains undergo successive active/dormant cycles that minimize radical termination processes and lead to a simultaneous growth of all chains.

Nowadays, the combination of metallic species with polymeric materials is a research area receiving much attention, due to the possibility of preparing variety of complexes. There are many reports revealing the oligomeric and polymeric coatings used for stabilization or further functionalization of magnetite nanoparticles.

Such hydrophobic manetite nanoparticles usually have to be transferred into water in most biomedical applications. This can be achieved by applying for specific designed amphiphilic polymer coating with a hydrophobic inner layer stabilize magnetite nanoparticles and a hydrophilic outer layer to make nanoparticles uniformly dispersed in water. Many researchers have attempted to prepare dispersed amphiphilic polymer-coated magnetite complexes. As cited literatures, there have been reported just a few research groups fucusing on the synthesis of amphiphilic polymer by RAFT polymerization for coating mangnetite nanoparticles. Due to ability to modify the end-group functionalities of RAFT polymer to bioconjugate to many biological compounds such as antibody and DNA, a search of a new kind of amphiphilic polymer by RAFT has been more interesting and challenging.

1.2 Objectives of research

1. To synthesize and characterize a novel amphiphilic polymer
2. To form amphiphilic polymer-coated magnetite dispersion

1.3 Scope of research

This research aims to synthesize the amphiphilic copolymers, hydrophobic aliphatic hydrocarbon and hydrophilic ethylene glycol type using RAFT polymerization and to prepare the monodispersed magnetite nanoparticles using thermolysis method of FeO(OH) precursor and finally, to form amphiphilic polymer-coated magnetite dispersion.

CHAPTER II

THEORY AND LITERATURE REVIEWS

2.1 Theory

2.1.1 Conventional free-radical polymerization

Conventional free-radical polymerization is defined as chain polymerization is initiated by a reactive species produced from an initiator. As shown in Scheme 2.1, the reactive species, which is as free radical, add to a monomer molecule by opening the π bond to form a new radical. The process is repeated as many more monomer molecules are successively added to continuously propagate the reactive center. Polymer growth is terminated at some point by destruction the reactive center by an appropriate reaction depending on the type of reactive center and the particular reaction condition.

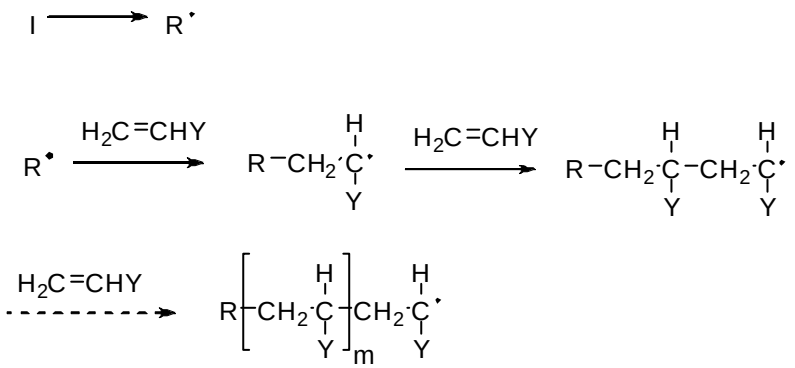

Scheme 2.1 Mechanism of conventional free-radical polymerization

Conventional free-radical polymerization is well known as one of the important commercial processes because it can be employed of many vinyl monomers under mild reaction conditions. In addition, many monomers can easily copolymerize

via this route, leading to an infinite number of copolymers with properties dependent on the proportion of the incorporated monomers. The main limitation of conventional free-radical polymerization is insufficient control over some of the key elements of macromolecular structures such as molecular weight (MW), polydispersity, end functionality, chain architecture, and composition [19].

2.1. 2 Living radical polymerization

Chain polymerizations without chain-breaking reaction, referred to as living polymerization would be highly attractive because they would allow the synthesis of block copolymers by the sequential addition of different monomers. A reactive species initiates polymerization of monomer. When the polymerization of monomer is complete, the reactive centers are intact because of no chain-breaking reactions. Addition of a second monomer results in the production of a block copolymer containing a long block of previous monomer repeat units followed by a long block of later monomer repeat units. It is possible to continue the sequential propagation by feeding a third batch of monomer, or one can terminate the process by the addition of a reagent to terminate the propagating centers [20].

The situation is very different for conventional radical polymerizations since the lifetime of propagating radicals in these systems is very short because of the ever-present occurrence of normal bimolecular termination by coupling and/or disproportionation. Living radical polymerizations have been accomplish by minimizing normal bimolecular termination and prolonging the lifetime of living polymers into hours or longer through the introduction of dormant states for the propagating species. This is acomplish through alternate modes of reaction for the propagating radicals, specifically, by either reversible termination or reversible transfer. Living radical polymerizations have good commercial potential for materials synthesis because many more monomers undergo radical polymerization compared to ionic polymerization

Living radical polymerizations include atom-transfer radical polymerization (ATRP) and stable free-radical polymerization (SFRP), which ran with reversible termination, and reversible addition–fragmentation transfer (RAFT), which proceeds with reversible chain transfer. Until the extensive exploration of these living polymerizations starting in the mid 1990s, radical polymerization was thought to be a mature process with relatively little left to discover. There is an ongoing effort to exploit the synthetic possibilities of living radical polymerization. Much of the driving force for the effort derives from the belief that well-defined materials from living radical polymerization will offer substantial advantages to build nanostructures for microelectronics, biotechnology, and other areas.

2.1.2.1 Atom-Transfer Radical Polymerization (ATRP)

Radical generation in atom-transfer radical polymerization involves an organic halide bearing a reversible redox process catalyzed by a transition metal compound such as cuprous halide. ATRP proceeds as described in Scheme 2.2 where L is as ligand that complexes with the cuprous salt and helps to solubilize it in the organic reaction system. Activation of the initiator involves the CuBr metal center undergoing an electron transfer with simultaneous halogen atom abstraction and expansion of its coordination sphere. R is the reactive radical that initiates polymerization. $CuBr_2(L)$ is the persistent radical that reduces the steady-state concentration of propagating radicals and minimizes normal termination of living polymers. The initiator and persistent radical are also called the activator and deactivator, respectively. At higher molecular weights normal bimolecular termination becomes significant especially at very high conversion and results in a loss of control. There also appears to be slow termination reactions of Cu^{2+} with both the propagating radicals and polymeric halide [21].

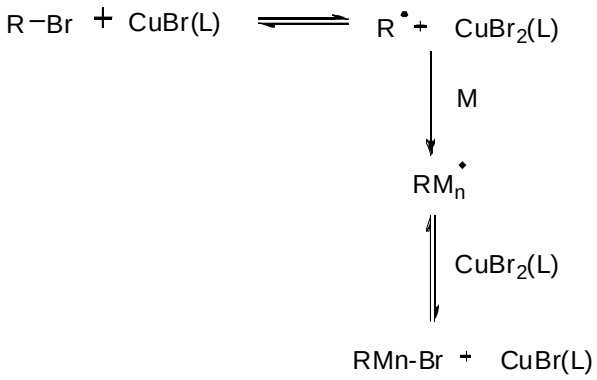

Scheme 2.2 Mechanism of atom-transfer radical polymerization

2.1.2.2 Stable Free-Radical Polymerization (SFRP)

Various stable radicals such as nitroxide, triazolinyl, trityl, and dithiocarbamate have been used as the mediating or persistent radical (deactivator) for SFRP. Nitroxides are generally more efficient than the others. Cyclic nitroxide radicals such as 2,2,6,6-tetramethyl-1-piper-idinoxyl (TEMPO) have been extensively studied. SFRP with nitroxides is called nitroxide-mediated polymerization (NMP). For example, one method involves the thermal decomposition of an alkoxyamine such as 2,2,6,6-tetramethyl-1-(1-phenylethoxy)piperidine into a reactive radical and a stable radical as shown in Scheme 2.3

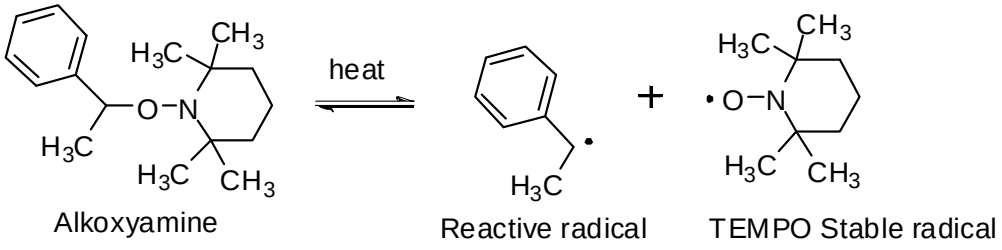

Scheme 2.3 Thermal decomposition of an alkoxyamine

The reactive radical initiates polymerization while the stable radical mediates the reaction by reacting with propagating radicals to lower their concentration. The

overall process as shown in Scheme 2.4 is analogous to ATRP. The nitroxide radical, although unreactive with itself, reacts rapidly with the propagating radical to decrease the concentration of propagating radicals sufficiently that conventional bimolecular termination is negligible. The propagating radical concentration is much lower than that of the dormant species; specifically and this results in living radical polymerization with control of molecular weight and molecular weight distribution [22]. NMP has some advantages and disadvantages compared to ATRP. A wide range of initiators (organic halides) are readily available for ATRP. Relatively few initiators for NMP, either nitroxides or alkoxyamines, are commercially available. The initiators need to be synthesized. K is generally larger for ATRP compared to NMP and is more easily adjusted by changing the initiator, transition metal, and ligands. Larger K values mean faster polymerization and milder reaction conditions. On the other hand, ATRP requires a relatively large amount of metal (0.1–1% of the reaction mixture) that needs to be removed from the final polymer product. In both NMP and ATRP, control of the reaction through establishment of a steady-state concentration of radicals is achieved by the balance between activation and deactivation. Conventional radical polymerization involves a balance between the rates of initiation and termination.

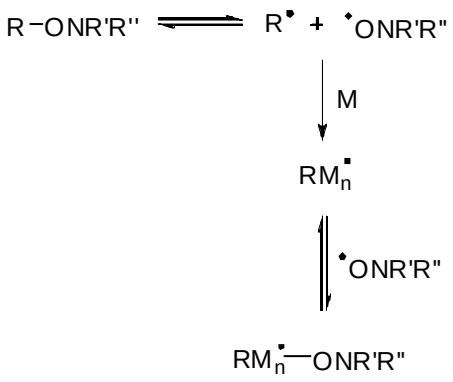

Scheme 2.4 Mechanism of stable free-radical polymerization (SFRP)

2.1.2.3 Radical Addition–Fragmentation Transfer (RAFT)

RAFT living polymerizations control chain growth through reversible chain transfer. A chain-transfer agent reversibly transfers a labile end group (a dithioester end group) to a propagating chain. The polymerization is carried out with a conventional initiator such as a peroxide or AIBN in the presence of the chain-transfer agent. The key that makes RAFT a living polymerization is the choice of the RAFT transfer agent. In addition, the transfer reaction in RAFT is not a one-step transfer of the labile end group, but involves radical addition to the thiocarbonyl group of the dithioester which functions as RAFT transfer agent to form an intermediate radical that fragments to yield a new dithioester and new radical [23].

Since RAFT is an essentially conventional radical polymerization conducted in the presence of a RAFT transfer agent, initiation can be accomplished with traditional initiators such as azo compounds, peroxides, redox initiating systems, photoinitiators and radiation. The primary radical, was generated by initiator, is generally believed to add to monomer prior to addition to the RAFT transfer agent due to the high relative concentration of monomer to RAFT transfer agent. For most RAFT polymerizations, the concentration of initiator relative to RAFT transfer agent is kept low to ensure a majority of the chains are initiated by RAFT transfer agent fragments (R•) as initiator-derived chains have a negative effect on the control of the molecular weight of the resulting polymer. Additionally, due to the exponential decomposition of conventional thermal initiators, primary radicals are continuously produced throughout the polymerization possibly leading to bimolecular termination. The continuous production of radicals also has the beneficial effect of replenishing any radicals lost to termination events and aids in maintaining reasonable polymerization rates.

RAFT polymerization proceeds with narrow molecular weight distributions as long as the fraction of chains terminated by normal bimolecular termination is small because a RAFT agent with high transfer constant is used and the initiator concentration decreases faster than does the monomer concentration. A significant

advantage of RAFT is that it works with a wider range of monomers than NMP and ATRP. RAFT does not produce polymers with copper or other metal present.

2.1.2.3.1 RAFT mechanism

As shown in Scheme 2.5, after reaction of the primary radical (I•) with monomer to give a propagating oligomeric chain (P_m•), the RAFT transfer agent reacts with P_m• to give an intermediate radical. This intermediate radical can fragment to yield the RAFT transfer agent and P_m•, or, if the correct RAFT transfer agent is chosen, fragmentation to form a polymeric macro-chain transfer agent and a new radical species, R•, is favored. The pre-equilibrium is defined as the time required for all R• fragments to add monomer units to form propagating chains. In order to achieve narrow molecular weight distributions, the pre-equilibrium must be completed early in the reaction for all the chains to enter the main equilibrium at the same time. This is analogous to other living polymerization systems in which initiation is assumed to occur quantitatively and instantaneously. Once the pre-equilibrium is complete, the polymerization enters the main equilibrium. This stage involves the degenerative transfer of the thiocarbonylthio end group between propagating chains through the formation and fragmentation of an intermediate radical. The exchange between active and dormant chains is established by the rapid fragmentation of the intermediate radical in both directions allowing for the controlled, intermittent addition of monomer to each chain with equal probability [24].

Most monomer consumption occurs during the main equilibrium and the number of monomer additions can vary depending on reaction conditions. It has been suggested, however, that for most RAFT polymerizations, less than one monomer is added to the propagating chains per transfer step. As in all “living” polymerization techniques, RAFT works to limit the number of irreversible termination events by minimizing the instantaneous concentration of radicals available for termination. As in all free radical processes, however, termination events occur through radical coupling and disproportionation and can be directly related to the starting initiator concentration. When the primary mode of termination is bimolecular combination, the

number of dead chains is equal to half the number of initiator-derived chains. In the case where disproportionation is the dominant mode of termination, the number of dead chains is equal to the total number of initiator derived chains. Termination of the intermediate radicals through radical coupling and disproportionation has also been shown, but the experimental conditions were not typical for RAFT polymerizations.

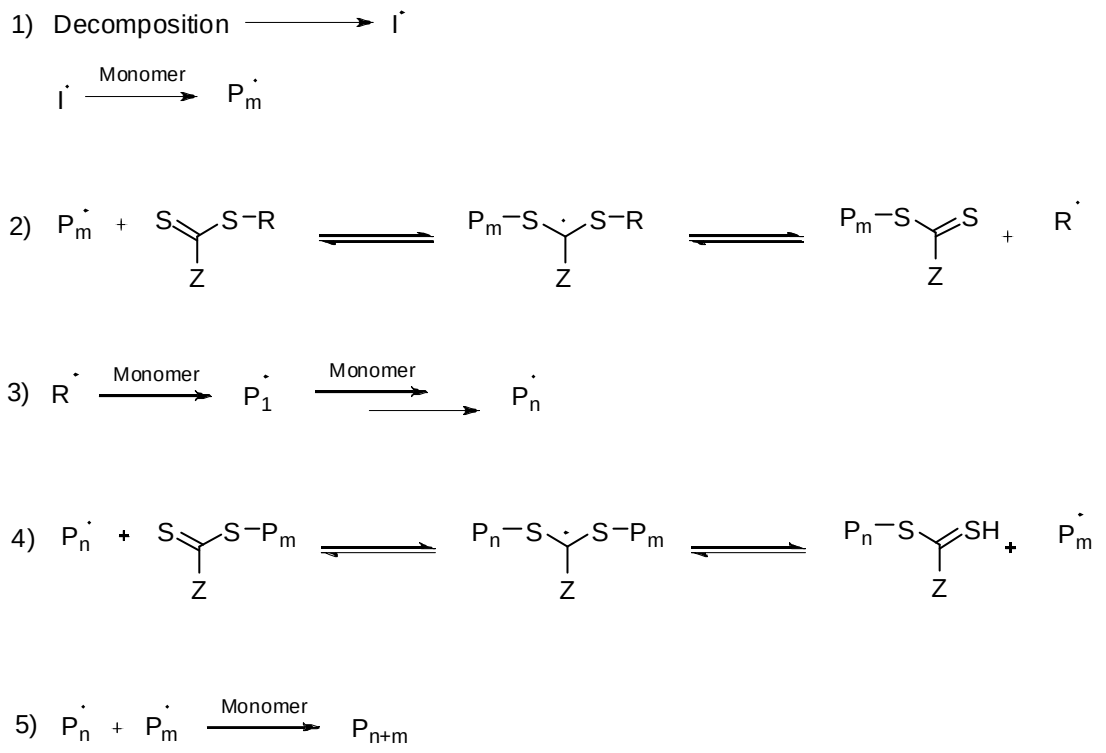

Scheme 2.5 RAFT mechanism

2.1.1.2.3.2 RAFT Agents

The structure of the R and Z groups are of the main factors to a successful RAFT polymerization. The R group of a RAFT agent is important in the pre-equilibium stage of the polymerization. The R group should be a better leaving group than the propagating radical and must efficiently reinitiate monomer as an expelled radical [25]. The Z group of a RAFT agent is highly influential in determining its reactivity and consequently its effectiveness at mediating polymerization. The Z

group should be chosen so that it will activate the C=S bond toward radical addition and then impart minimal stabilization of the adduct radical formed [26].

If the stabilizing effect of the Z group is too high, fragmentation may not be favored and inhibition of the polymerization (in the initial step) or retardation (in the main process) might be observed. More reactive monomers are better controlled by RAFT agents that have a lesser activating effect on the thiocarbonyl group and, therefore, a greater destabilizing effect on the adduct radical, thus favoring fragmentation. The adduct radical formed by a more reactive monomer is more stable and less likely to undergo fragmentation. Thus, a Z group that destabilizes the adduct radical is required so that fragmentation can occur.

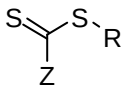

RAFT chain transfer agent

2.1.3 Polymer purification methods

2.1.3.1 Dialysis method

Polymer can be separated from oligomers or small organic molecules by dialysis through a semipermeable membrane, such as a cellulose membrane with pores as shown in Figure 2.1. Dialysis is the diffusion of dissolved solutes across a selectively permeable membrane against a concentration gradient in an effort to achieve equilibrium. While small solutes pass through the membrane larger solutes are trapped on one side. By exchanging the dialysate buffer or water on the outside side of the membrane, the smaller solutes can continually be pulled away to purify the trapped larger molecules. In general, dialysis will be most effective when the buffer or water is replaced a few times over the course of a day and then left overnight at room temperature on a stir plate. A standard protocol for dialysis is 16 to 24 hours. Many factors affect the rate dialysis, including: diffusion coefficients, pH, temperature, time, concentration of species, sample volume, dialysate (buffer) volume, number of

dialysate changes, membrane surface area, membrane thickness, molecular charges and dialysate agitation

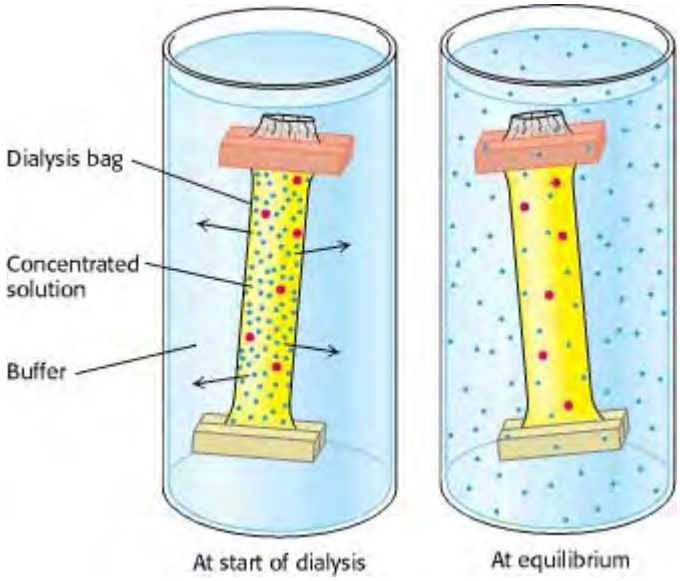

Figure 2.1 Dialysis method, which polymer (red) are retained within the dialysis bag, whereas small molecules (blue) diffuse into the surrounding medium.

2.1.3.2 Precipitation method

Polymer can be purified to remove monomers and some organic molecule by precipitation technique. The suitable solvent for precipitation of polymer should be able to dissolve monomers and other organic molecules except polymer. Because of high molecular weight of polymer, polymer is also more difficult to be dissolved in solvent. This technique is well-known as common and simple technique to use for purification of polymer

2.1.4 Polymer characterization

2.1.4.1 Gel Permeation Chromatgraphy (GPC)

Gel Permeation Chromatgraphy (GPC), also known as Size Exclusion Chromatography (SEC) is a technique use to determine the average molecular weight distribution of a polymer sample. Using the appropriate detectors and analysis procedure it is possible to obtain qualitative information on long chain branching or determine the composition distribution of copolymer.

As the name implies, GPC or SEC separates the polymer according to size or hydrodynamic radius. This is accomplished by injecting a small amount (100-400 µl) of polymer solution (0.01-0.6%) into a set of columns that are packed with porous beads. Smaller molecules can penetrate the pores and are therefore retained to a greater extent than the larger molecules which continue down the columns and elute faster. One or more detectors is attached to the output of the columns. For routine analysis of linear homopolymers, this is most often a Differential Refractive Index (DRI) or a UV detector. For branched or copolymer, however, it is necessary to have at least two sequential detectors to determine molecular weight accurately. The compositional distribution of copolymers, i.e., average composition as a function of molecular size, can be determined using a DRI detector coupled with a selective detector such as UV or FTIR. It is important to consider the type of polymer and information that is desired before submitting a sample. The following outline describes each instrument that is currently available.

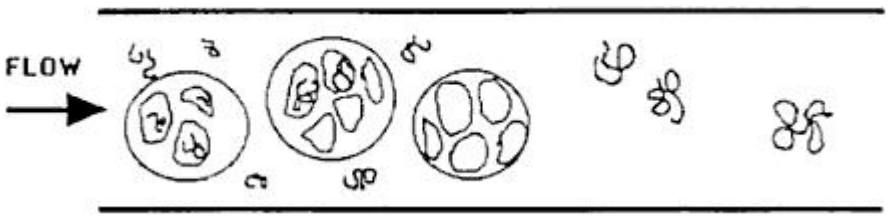

Figure 2.2 Polymer solution flow though GPC column

2.1.4.2 Attenuated total reflection fourier transform infrared spectroscopy (ATR-FTIR)

Infrared spectroscopy can be used in reflection or attenuated total reflection mode (ATR-FTIR) for surface and thin film investigations. As a spectroscopic technique it also allows quantitative determination of composition or binding states *via* vibrational modes and is a powerful analytical tool for the molecular detection of dynamics at the solid or solid/ air interface between this crystal and the surrounding medium is investigated. At the interface the IR beam is totally by reflected, but still penetrates into the surrounding medium. Different materials can be distinguished by their IR spectrum and deuteration is sometimes used to enhance contrast between components. The penetration depth of the evanescent wave is of the order of wavelength and the technique therefore probes a depth of several micrometers. With an IR microscope a sample can be scanned directly imaged but lateral resolution is typically determined by the wavelength of the radiation. Scan speed and imaging is highly facilitated by use of an IR array detector where spectroscopic information is obtained at high spatial resolution, but also allows us to utilize IR ellipsometric imaging techniques for the measurement of composition, orientation, thickness and index of refraction of thin film surfaces.

2.1.4.3 Thermogravimetric analysis (TGA)

Thermal analysis refers to variety of techniques in which a property of a sample is continuously measured as the sample is programmed through a predetermined temperature profile. Among the most common technique is thermal gravimetric analysis (TGA). TGA makes a continuous weighing of a small sample in a controlled atmosphere (e.g., air or nitrogen) as the temperature is increase at a programmed linear rate. A thermogram as shown in Figure 2.3 illustrates weight losses due to desortion of gases (e.g., moisture) or decomposition (e.g., HBr loss from halobutyl, CO_2 from calcium carbonate filler). Thermal analysis is a very simple technique for quantitative analyzing for filler content of a polymer compound. While oil can be readily detected in the thermogram it almost always overlaps with the

temperature range of hydrocarbon polymer degradation. The curves cannot be reliably deconvoluted since the actual decomposition range of a polymer in a polymer blend can be affected by the sample morphology.

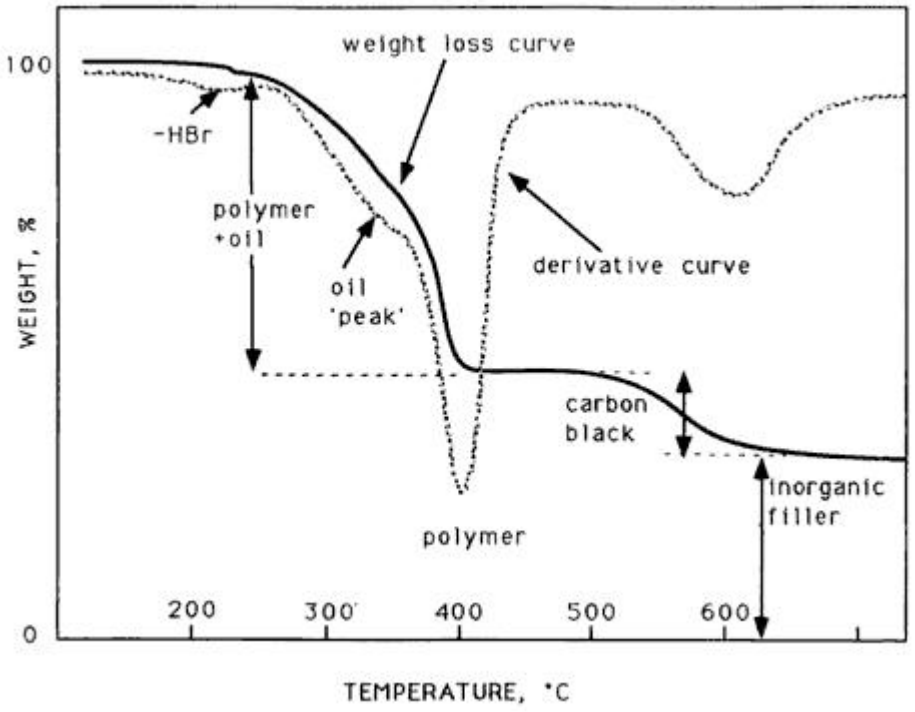

Figure 2.3 Sample thermogram of TGA

2.1.4.4 Nuclear magnetic resonance spectrometry

Nuclear magnetic resonance (NMR) is a spectrometric technique for determining chemical structures. When an atomic nucleus with magnetic moment is placed in a magnetic field, it tends to align with the applied field. The energy required to reverse this alignment depends on the strength of the magnetic field and to a minor extent on the environment of the nucleus, i.e., the nature of the chemical bonds between the atom of interest and its immediate vicinity in the molecule. This reversal is a resonant process and occurs only under select conditions. By determining the energy levels of transition for all of the atoms in a molecule, it is possible to determine many important features of its structure. The energy level can be expressed

in terms of 500-600 MHz for high magnetic fields. The minor spectral shifts due to chemical environment are the essential features for interpreting structure and are normally expressed in terms of part-per-million shifts from the reference frequency of a standard such as tetramethyl silane.

The most common nuclei examined by NMR are ^{1}H and ^{13}C, as these are the NMR sensitive nuclei of the most abundant elements in organic materials. ^{1}H represents over 99% of all hydrogen atoms, while ^{13}C is only just over 1% of all carbon atoms; feature, ^{1}H is much more sensitive than ^{13}C on an equal nuclei basis. Until fairly recently, instruments did not have sufficient sensitivity for routine ^{13}C NMR, and ^{1}H was the only practical technique.

In general, the resonant frequencies can be used to determine molecular structures. ^{1}H resonances are fairly specific for the types of carbon they are attached to, and to a lesser extent to the adjacent carbons. These resonances may be split into multiples, as hydrogen nuclei can couple to other nearby hydrogen nuclei. The magnitude of splitting, and the multiplicity, can be used to better determine the chemical structure in the vicinity of given hydrogen. When all of the resonance observed are similarly analyzed, it is possible to determine the structure of the molecule. However, as only hydrogen is observed, any skeletal feature without an attached hydrogen can only be inferred. Complications can arise if the molecule is very complex, because then the resonances can be overlaps severely and beome difficult or impossible to resolve.

^{13}C resonance can be used to directly determine the skeleton of an organic molecule. The resonance lines are narrow and the chemical shift range (in ppm) is much larger than for ^{1}H resonances. Furthermore, the shift is dependent on the structure of the molecule for up to three bonds in all directions from the site of interest. Therefore, each shift becomes quite specific, and the structure can be easily assigned, frequently without any ambiguity, even for complex molecules.

Very commonly, however, the sample of interest is not a pure compound, but it is a complex mixture such as a coal liquid. As a result, a specific structure determination for each molecule type is not practical, although it is possible to determine an average chemical structure. Features which may be determined include the hydrogen distribution between saturate, benzylic, olefinic, and aromatic sites. The carbon distribution is usually split into saturate, heterosubstituted saturate, aromatic, olefinic, carboxyl, and carbonyl types. More details are possible, but depend greatly on the nature of the sample, and what information is desired.

Any gas liquid or solid sample that can be dissolved in solvents, such as CCl_4, CH_3Cl, acetone or DMSO to the one percent level or greater can be analyzed by this technique. Sample of 0.1 g or larger of pure material are sufficient for analysis by thtechnque. Solids can also be analyzed as solid. However, special arrangements need to be made. In either case, the analysis is non-destructive so that samples can be recovered for further analysis if necessary.

The NMR experiment can be conducted in a temperature range from liquid nitrogen (-209 ^{o}C) to +150 ^{o}C. This gives the experimenter the ability to slow down rapid molecular motions to observable rates or to speed up very slow or viscous motions to measurable rates.

NMR is very powerful tool. It often provides the best characterization of compound structure, and may provide absolute identification of specific isomers in simple mixtures. It may also provide a general characterization by functional groups which cannot be obtained by any other technique. As it typical with many spectroscopic methods, adding data from other techniques, such as mass or infrared spectrometry) can often provide greatly improved characterizations.

2.1.5 Magnetic magnetite nanoparticles

Magnetic nanoparticles, a class of inorganic nanocrystal, have been of great interest not only as contrast agents for magnetic resonance imaging (MRI) but also

more recently as drug-delivery vehicle in cancer therapy and have been used in many applications in nanotechnology and biomedical. Due to the approval in *vivo* applications of the use of magnetite nanoparticles by FDA, much work has been intensively studied for the use as contrast agents for magnetic resonance imaging [7], drug/ gene delivery [9], biosensor and hyperthermia treatment of cancer [27].

Magnetite (Fe_3O_4) nanoparticles offers high potential for advancements in electronics, magnetic storage, biomedical, ferrofluid, separation and magnetically guided drug carriers for targeting the therapy [28]. Recently, synthesis of magnetic materials at nanoscale has been a topic of subject in nanotechnology. In fact, the control of the monodisperse size of magnetite nanoparticles has been focused on many research studies because the properties of the nanoparticles strongly depend upon the dimension and size of the nanoparticles. Magnetite nanoparticles with appropriate surface chemistry can be used for numerous *in* vivo applications. For example, magnetite nanoparticles with appropriate surface can bind to drugs, proteins, enzymes, antibodies, or nucleotides and also be directed to an organ, tissue, or tumor using an external magnetic field.

2.1.5.1 Synthesis of magnetite nanoparticles

The synthesis of magnetite nanoparticles has been paid much attention not only for its fundamental scientific interest but also for many technological applications: magnetic storage media, biosensing applications, medical applications, such as targeted drug delivery, contrast agents in magnetic resonance imaging (MRI), and magnetic inks for jet printing. The synthesis of magnetite nanoparticles, covering a wide range of turnable sizes, has been made substantial progress, especially over the past decade. Different kinds of monodisperse spherical nanopaticles with control label particle sizes have been synthesized by a wide range of chemical synthetic procedures. As cited literatures, synthesis of magnetite nanoparticles can be achieved through various methods such as co-precipitation, microemulsion, thermolysis of organic compounds and a reduction of metal salts in aqueous solution. However,

search in advance synthetic methods have been challenged for the preparation of a wide range of highly crystalline and uniformly sized magnetite nanoparticles.

There are several methods to produce magnetic magnetite nanoparticles. Some of mainly techniques for the formation of magnetite nanoparticles are explained as follows:

2.1.5.1.1 Co-precipitation method

The co-precipitation technique is the simplest and most efficient pathway to produce magnetite nanoparticles. Magnetite is usually prepared by an aging stoichiometric mixture of ferrous and ferric salts as the following equation 1

$$Fe^{3+} + 2Fe^{2+} + 8OH^- \longrightarrow Fe_3O_4 + 4H_2O \quad \text{.....(1)}$$

It would recommend that the complete precipitation of magnetite should be performed in a range of pH 8 and 14 under a non-oxygenated condition [29]. However, magnetite is very sensitive to be oxidized and can be converted to maghemite under air atmosphere. Not only air oxidation but it is also the acidic reaction condition which could transform magnetite to maghemite. The main advantage of the co-precipitation is a large amount of magnetite nanoparticles can be synthesized. However, the limitation of this technique is hardly to control the particle size of the particles. There are two stages mainly involved in co-precipitation technique. A short burst of nucleation occurs when the concentration of the species reach to critical supersaturation and then a slow growth of nuclei is formed by the diffusion of the solute to the surface of the crystal.

2.1.5.1.2 Hydrothermal and high-temperature reaction method

Hydrothermal and high-temperature are performed in aqueous media in reactors or autoclaves where the pressure can be higher than 2000 psi and the temperature can be above 200 ^{o}C. Well monodispersity and size control of magnetite

nanoparticles can be prepared by high-temperature decomposition of iron organic precursors, such as $Fe(Cup)_3$, $Fe(CO)_5$, or Fe(acac) [30]. Two main route are involved for the formation of magnetite via hydrothermal conditions: hydrolysis and oxidation or neutralization of mixed metal hydroxides. Many parameters such as solvent, temperature and time can be affected to the production of magnetite. For example, the particle size of magnetite increased with a prolonged reaction time and higher water content resulted in the precipitation of larger magnetite. To control the particle size of magnetite, it is mainly through the rate processes of nucleation and grain growth. When nucleation is faster than gain growth at higher temperatures, it could result in a decrease in particle size of magnetite.

2.1.5.1.3 Sol-Gel reactions method

The sol-gel reaction is based on the hydroxylation and condensation of molecular precursors in a solution. This method is a versatile approach for the synthesis of nano- and microparticles with well defined shapes and controlled size. In fact, a three dimensional metal oxide network denominated wet gel after condensation and inorganic polymerization [31]. The properties of a gel are very dependent upon the structure created during the sol stage of the sol-gel process. The main parameters that influence the kinetics, growth reaction, hydrolysis, condensation reaction are solvent, temperature, concentration of the precursors, pH and atmospheres [32].

2.1.5.1.4 Sonolysis method

Sonolysis of organometalic precursors such as $Fe(CO)_5$ can prepare magnetite nanoparticles. The very high temperature hot spot generated by the rapid collapse of sonically generated cavities space for the conversion of ferrous salts into magnetite nanoparticles. Polymer, organic capping agents or structure hosts are used to limit growth of the particle formation. If stabilizer or polymers are added during sonication or after sonication, metal colloids could be produced [33].

2.1.5.2 Modified coating surface on magnetite nanoparticles

As the matter of fact, magnetite is extremely unstable and is sensitive to oxidation in air and could be turned into maghemite. To prevent these obstacles, most synthetic methods are required to modify surface of magnetite or coat nanoparticles with organic materials, such as biomaterials and polymers, to produce an electrostatic or steric repulsive force [34-38]. In biomedical applications, it is required the nanoparticles have high magnetization values, a size smaller than 100 nm, and a narrow particle size distribution. These applications also require peculiar surface coating of the magnetic particles, which has to be nontoxic and biocompatible and must also allow for a targetable delivery with particle localization in a specific area. Several approaches have been developed to coat magnetite, including in situ coatings and post-synthesis coating. For example, dextran, a polysaccharide polymer composed of glucopyranuosyl units, has been used often as a polymer coating magnetite mostly because of its biocompatible and the high bonding energy of hydrogen bonds over the chain length of polymer [39]. Several studies were reported the use of polyethylene glycol to increase the biocompatibility of magnetite dispersions and blood circulation times due to its properties as hydrophilic, water-soluble, biocompatible polymer [40-41].

2.2 literature reviews

Nowadays, the combination of metallic species with polymeric materials is a research area receiving much attention, due to the possibility of preparing variety of complexes. There are many reports revealing the oligomeric and polymeric coatings used for stabilization or further functionalization of magnetite nanoparticles.

In 2009, Amstad *et al*. [34] investigated the effect of eight different catechol-derivative anchor groups on poly(ethylene glycol) (PEG), with molecular weight of 5 kDa (PEG(5)), on the stability of magnetite nanoparticles. In addition, 6 nm of magnetite core was prepared by the microwave-assisted nonaqueous sol-gel. PEG(5)-hydroxypyrone and PEG(5)-COOH stabilized magnetite nanoparticles formed

agglomerates larger than 200 nm in diameter. As for PEG(5)- nitroDOPA, PEG(5)-nitrodopamine, PEG(5)-mimosine, PEG(5)-DOPA, PEG(5)-dopamine, PEG(5)-hydroxydopamine,and PEG(5)-hydroxypyridine stabilized magnetite nanoparticles, they showed good stability in 4-(2-hydroxyethyl)-1-piperazineethanesulfonic acid (HEPES) containing 150 mM NaCl, pH = 7.4 at room temperature or could alternatively redispersed in millipore water and stored for at least 4 months without noticeable change. In additions, their diameter was observed around 23 nm.

In 2009, Yang *et* al. [42] report a novel and facile approach to the fabrication of superparamagnetic magnetite/poly(styrene-co-12-acryloxy-9-octadecenoic acid) nanocomposite microspheres with controllable structure *via* γ-ray radiation induced inverse emulsion polymerization under room temperature and at ambient pressure. 12-Acryloxy-9-octadecenoic acid (AOA), containing part of sodium salts Na–AOA, as a surfactant can also copolymerize with the styrene. It is interesting that just by changing the added amount of styrene, the magnetic hollow spheres with different wall thickness and various sizes of core, up to the magnetic solid spheres, can be obtained. The overall synthetic procedure is shown in Scheme 2.6. The γ-ray is chosen to induce the polymerization of monomer due to the reactions at low temperature, which is useful to keep the stability of inverse emulsion during polymerization.

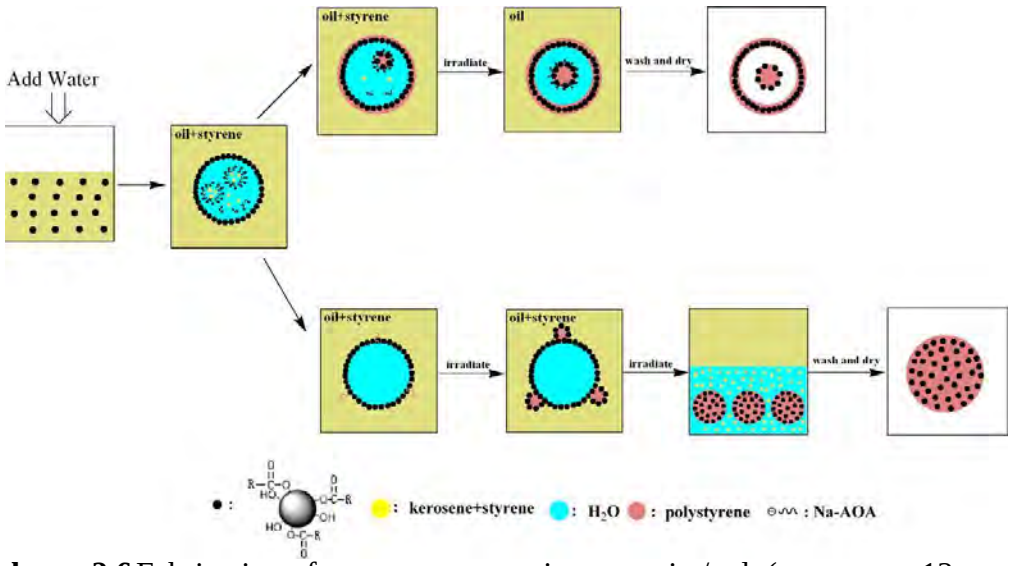

Scheme 2.6 Fabrication of superparamagnetic magnetite/poly(styrene-*co*-12-acryloxy-9-octadecenoic acid) nanocomposite microspheres with controllable structure.

In 2009, Podzus *et* al. [43] revealed a success of the synthesis of chitosan magnetic microspheres. In addition, acetic acid (1% w/v) solution was used as solvent for the chitosan polymer solution (2% w/v) where magnetite nanoparticles were suspended in order to obtain a stable ferrofluid while glutaraldehyde was used as cross-linker. In figure 2.4, the morphological characterization of the microspheres shows that they can be produced in the size range 800–1100 mm. In addition, The adsorption of Cu(II) onto chitosan–magnetite nanoparticles was studied in batch system. A second-order kinetic model was used to fit the kinetic data, leading to an equilibrium adsorption capacity of 19 mg Cu/g chitosan.

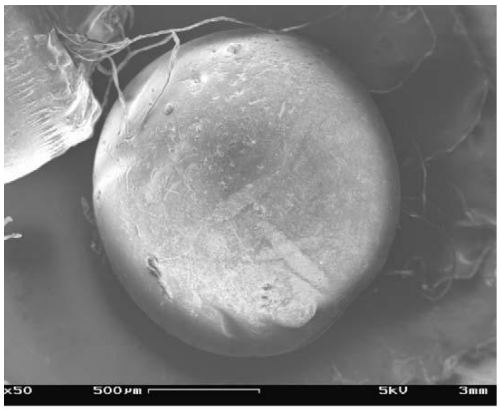

Figure 2.4 Scanning electron micrographs (SEM) of cross-linked magnetic micro- spheres

In 2009, Moolekamp *et* al. [44] investigated the formation of colloidal gold and magnetite (Fe_3O_4) nanoparticles which were chemically linked using a bifunctional organic ligand creating clusters of the two nanoparticle components. The linked gold-magnetite clusters were blended with a transparent polymer and cast as films. Three samples were produced with a different ratios of 30 nm gold and 8 nm magnetite nanoparticles. The localized surface plasmon peak of the gold nanoparticles observed in the optical absorption data at 538 nm. Spectral Faraday rotation and ellipticity data show changes in both spectra which correlate to this surface plasmon resonance wavelength. Specifically, the inclusion of gold nanoparticles results in a change in sign of the Faraday rotation as well as an enhancement of the ellipticity of about 1.8 in the spectral region corresponding to the surface plasmon absorption peak of the gold nanoparticles.

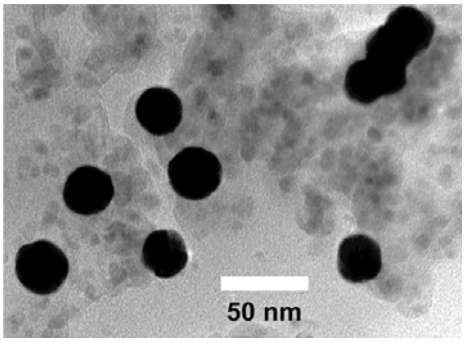

Figure 2.5 Transmission electron micrograph of the gold-magnetite composites: The darker spheres are 30 nm gold particles.

In 2010, Abdalla *et* al. [45] reported a success of the synthesis of noscapine containing magnetic polymeric nanoparticles using ironoxide nanoparticles, and two FDA approved polymeric systems—polylactide acid (PLLA) and poly (l-lactide acid-co-gylocolide) (PLGA). The average size of prepared NMNP was about 250 nm which is well within the acceptable range for the solvent evaporation/extraction technique in oil in water emulsion method. FT-IR spectra of PLLA, noscapine, and NMNP showed the encapsulation of the drug on the polymer surface while elemental analysis confirmed the presence of the Fe_3O_4 NPs on the surface of the prepared NMNP. The drug loading efficiency of the drug on the two polymeric systems was studied using HPLC and the drug entrapment was always higher in the case of PLLA or PLGA with the lower molecular weights. Higher values of no scapine entrapment on the low molecular weigh tpolymer were attributed to the favorable interaction between the noscapine methoxy groups and the higher number of free functional groups in the low molecular weight PLLA and PLGA.

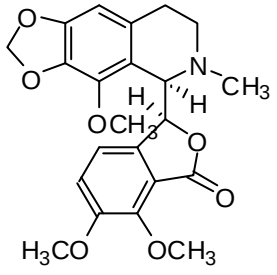

(S,R)-Noscapine

Figure 2.6 Structure of noscapine

In 2010, Miles *et al*. [35] reported the success of synthetic well-defined magnetite nanoparticles coated with tricarboxylate-functional polydimethylsiloxane (PDMS) oligomers using two different magnetite synthetic methods, co-precipitation method and thermolysis method. In co-precipitation method, synthetic iron oxide nanoparticles need to be separated due to large particle size distribution. Interestingly, nearly 80% of the total starting materials were lost in the separation process. As for thermolysis method, there is no need for magnetic fractionation because of a well-defined particle size distribution.

In 2010, Cha *et al*. [36] demonstrated the novel 2, 3-meso-dimercaptosuccinic acid (DMSA) surface-modified magnetite nanoparticles which were acclaimed as monodispersed nanocomplex with the average size of 12.5 nm. It was interesting that the core magnetite size of the complex was slightly smaller than the uncoated magnetite nanoparticles. This was expected that α–Fe_2O_3 phase would exhibit the phase deformation in interface layer between Fe_3O_4 nanoparticles and ligand.

In 2010, Yang *et* al. [46] reported a novel production of monodisperse magnetic polymer microspheres by combined swelling and thermolysis technique. As shown in Scheme 2.7, the monodisperse polystyrene microspheres were required to prepare first by dispersion polymerization and swelled into chloroform. Then, ferric oleate was inputed in chloroform as a precursor and impregnated into the swollen polymer microspheres. Subsequently, the magnetite nanoparticles were formed within the polymer matrix by thermal decomposition of ferric oleate. The results showed that the average diameter of the magnetic polymer microspheres was 5.1 μm with a standard deviation of 0.106.

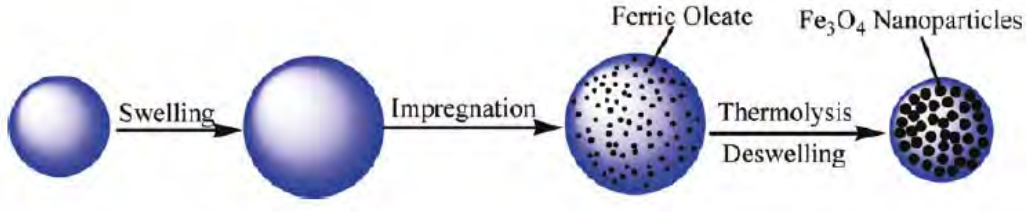

Scheme 2.7 Preparation of monodisperse magnetic polymer microspheres by swelling and thermolysis technique

In 2010, Basavaraja *et* al. [47] demonstrated the successful synthesis of poly(N-vinylcarbazole)-capped magnetite nanocomposite films by oxidative polymerization with capped magnetite nanoparticles for the preparation of conducting polymer composites. Characteristics of the composite films show an increase of the conductivity of poly(N-vinylcarbazole) film due to the presence of capped magnetite nanoparticles. In addition, the nanocomposites show an increased thermal stability, which can be interpreted because of the increase of nanoparticles which were chemically bonded to the polymeric chains.

In 2010, Kavas *et* al. [48] reported Poly(1-vinyl-1,2,4-triazole) (PVTri)–Fe_3O_4 nanocomposite with conducting and magnetic characteristics was successfully synthesized by wet chemical processes. PVTri has been synthesized in a separate process and was then coated/adsorbed on sonochemically synthesized magnetite nanoparticles. Crystallite size was calculated for magnetite by X-ray line profile fitting as 12 $\pm$ 6 nm. FT-IR and TGA analysis confirm the adsorption/coating of PVTri on magnetite nanoparticles. SEM micrographs in Figure 2.7 revealed that Fe_3O_4 nanoparticles are aggregated upon PVTri coating. Conductivity and permittivity measurements show the effect of glass transition temperature of polymer part in PVTri/Fe_3O_4 nanocomposite. At 150 ^oC, the AC conductivity values are enormously higher at this temperature than that of at lower temperatures. This temperature corresponds to the onset of glass transition temperature of the pristine PVTri host polymer and conductivity increase at this temperature may be because of contribution of ionic conductivity

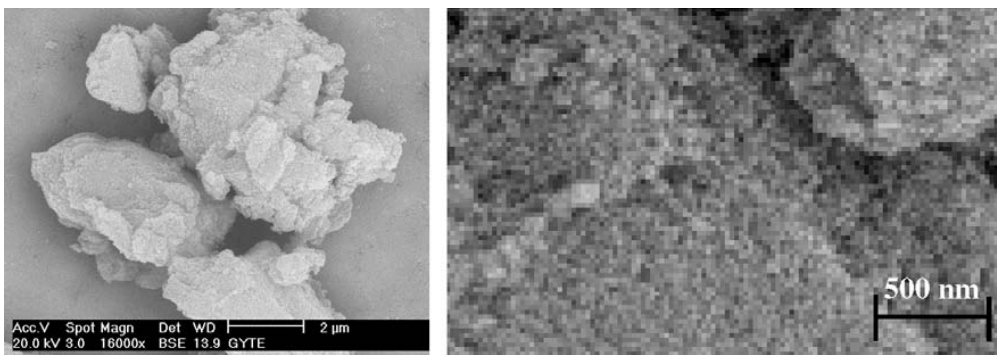

Figure 2.7 Scanning electron micrographs (SEM) of Fe_3O_4/PVTri nanocomposite

In 2010, Frickel *et* al. [49] reported the success of the preparation of single dispersed 3-methacryloxypropyl triethoxysilane(MTS)-modified magnetite particles which exhibit an averaged hydrodynamic diameter of 20.3 $\pm$ 1.3 nm. By selecting the functionality of alkoxysilanes, the surface properties of the particles can be tailored. Three kind of polymeric-coated MTS-magnetite nanoparticles, poly(methyl methacrylate) (PMMA) magnetic composites, Fe_3O_4@poly(N-isopropylacrylamide) hybrid particles and Fe_3O_4@poly[oligo-(ethyleneglycol)methylether methacrylate brush-coated nanoparticles were successfully prepared. Poly(methyl methacrylate) (PMMA) magnetic composites (Fe_3O_4*PMMA) are synthesized by a free radical polymerization, which MTS-modified Fe_3O_4 nanoparticles dispersed in MMA monomer with AIBN. The swelling degree of Fe_3O_4*PMMA composites in chloroform is found to be between 5 and 10 for networks with magnetite content in the solid between 2 and 10 mass indicating the contribution of the particles to cross-linking. Fe_3O_4@ Poly(N-isopropylacrylamide) hybrid particles were prepared by a grafting-through free radical polymerization process in the presence of N-isopropylacrylamide and AIBN. The polymer fraction of the materials according to elemental analysis is between 10 and 20 mass%, depending on the experimental conditions, and the growth in particle diameter indicated by dynamic light scattering compared to MTS-functional particles is between 4 and 6 nm. Magnetic Fe_3O_4@poly[oligo-(ethyleneglycol)methylether methacrylate brush-coated nanoparticles was successfully prepared by surface-initiated atom transfer radical polymerization (ATRP) in the presence of copper(I) bromide, oligo(ethyleneglycol) methylether methacrylate.

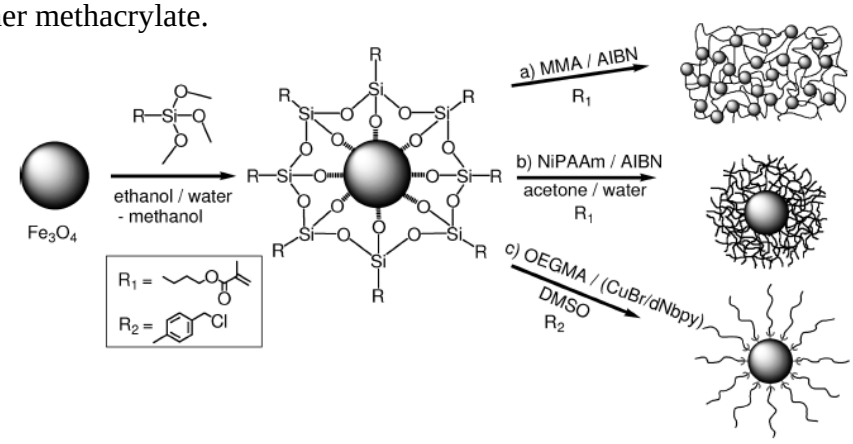

Scheme 2.8 Synthesis of magnetic polymer hybrid nanocomposites of different architecture

In 2010, Bhatt *et* al. [50] reported crystalline magnetite nanoparticles, hexagonal shape with weak agglomeration, were successfully synthesized by the hydrothermal process and also embedded in the chitosan polymer with different concentration of the polymer by ultrasonication route. The optical band gap values of the composites, was evaluated using the UV–visible Spectroscopy, showed a red shift, which confirmed the dispersion of the magnetic filler in the polymer matrix. The saturated magnetization of the composite films could reach a value of 10.31 emu/g with 50 % doping of magnetite. The impedance spectroscopy results showed the presence of nanoparticles eases the electron transfer between the solution and the electrode and the RCT value goes a slow as 8.23 ohms. The influence of magnetite content on the magnetic properties of the composite showed a decrease in the saturation magnetization with the decrease in the magnetic content.

In 2010, Hsiao *et* al. [51] demonstrated a new approach for preparation of Au-decorated magnetic Fe_3O_4/ PS/PMAA spheres as shown in Figure 2.9. Two essentials were distinguished for fabrication of this kind of hybrid composites. The first involves synthesizing surface functionalized magnetic polymer spheres using seeded growth polymerization based on emulsion emulsifier-free system. Oleate-stabilized magnetite nanoparticles having lyophobic property and super-paramagnetic structure with a saturation magnetization of 53 emu g^{-1} were successfully prepared using hydrothermal process. The magnetic Fe_3O_4/Polystylene spheres containing oleate-stabilized Fe_3O_4 nanoparticles were prepared by the suspension polymerization. In addition to styrene monomer and potassium persulfate, methyl acrylic acid was chosen as the second monomer in the seeded polymerization, in which dual functional groups present in the newly formed PMAA layer should result. The second performs self-reduction of Au nanoparticles onto magnetite/poly (methyl acrylic acid) spheres by expelling utilization of extra reducing agent.

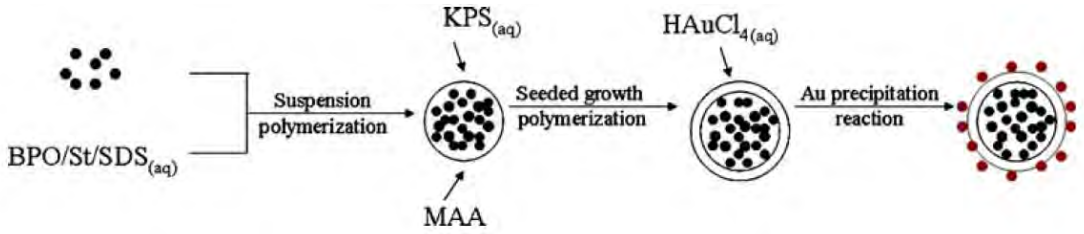

Scheme 2.9 Preparation of Au-decorated PMAA-coated magnetite/PS spheres

Such hydrophobic manetite nanoparticles usually have to be transferred into water in most biomedical applications. This can be achieved by applying for specific designed amphiphilic polymer coating with a hydrophobic inner layer stabilize magnetite nanoparticles and a hydrophilic outer layer to make nanoparticles uniformly dispersed in water. Many researchers have attempted to prepare dispersed amphiphilic polymer-coated magnetite complexes. For examples, Jain *et al.* [37] reported the successful synthesis of amphiphilic polymer-coated magnetite complex by using Pluronic, poly(ethylene oxide)-poly(propylene oxide) as polymeric shell. Lee *et al.* [38] reported the development of encapsulation of magnetite nanoparticles within their poly(D,L-lactic-co-glycolic acid) (PLGA) core and a hydrophilic glycol chitosan (GC) shell. However, there was significantly that PLGA resulting in loss of magnetization (40-50%) of the core magnetite. As cited literatures, there have been reported just a few research groups fucusing on the synthesis of amphiphilic polymer by RAFT polymerization for coating mangnetite nanoparticles. Due to ability to modify the end-group functionalities of RAFT polymer to bioconjugate to many biological compounds such as antibody and DNA, a search of a new kind of amphiphilic polymer by RAFT has been more interesting and challenging.

The focus of this study is a search of a new kind of amphiphilic polymer synthesized by RAFT polymerization. The synthetic polymers will be applied to coat well monodispersed magnetite nanoparticles resulting in the dispersed amphiphilic polymer-coated magnetite complex.

CHAPTER III

EXPERIMENTAL

3.1 General Procedure

Melting points were measured by a Fisher-Johns melting point apparatus and further uncorrected. The ATR-IR spectra were recorded on a Nicolet Fourier transform infrared spectrophotometer model Impact 410. The ^{1}H and ^{13}C-NMR spectra were obtained in deuterated chloroform ($CDCl_3$) solvent, with a Bruker model ACF200 spectrometer and Jeol, Model JNM-A500. High performance liquid chromatography was carried out using following equipments: Water 2414 RI. The column used for HPLC technique was Phenogel 500 A, Linear , 10E6A SET #1 with guard column. Thermal gravimetric analysis (TGA) 2950 were performed using TA Instruments Inc.

3.2 Chemicals

All chemical were of analytical grade and listed in Table 3.1. There were used without further purification unless otherwise note.

Table 3.1 Chemical list

Chemicals	Supplier
1. 1-Dodecanethiol	Aldrich
2. Tricaprylylmethylammonium chloride	Aldrich
3. Sodium hydroxide	Merck
4. Carbon disulfide	Merck

Chemicals	Supplier
5. Chloroform	Fisher Scientific
6. Hydrochloric acid, 37%	Merck
7. 2-propanol	Fluka
8. Hexane	Merck
9. Methanol	Merck
10. Dicyclohexylcarbodiimide	Aldrich
11. Dichlomethane	Merck
12. 4-Dimethylamino- pyridine	Aldrich
13. N-(2-hydroxyethyl)maleimide	Aldrich
14. 1-Octadecene	Aldrich
15. AIBN	Aldrich
16. Anhydrous 1,4-dioxane	Aldrich
17. Diethyl ether	Merck
18. Maleic anhydride	Aldrich
19. 2-(2-aminoethoxy)-ethanol	Aldrich
20. 1-ethyl-3-(3-dimethylaminopropyl) carbodiimide	Aldrich
21. *N*-hydroxysulfosuccinimide	Aldrich
22. Iron carboxylate salts, FeO(OH)	Aldrich
23. Oleic acid	Aldrich

3.3 Synthesis of RAFT agents

Two kinds of RAFT agents, S-1-Dodecyl-S′-(*α,α′*-dimethyl-*α″*-acetic acid)-trithiocarbonate (DDMAT) and S-1-Dodecyl-S′-(*α,α′*-dimethyl-*α″*-methyl acetate)-trithiocarbonate (DDMMAT) were synthesized as follows:

3.3.1 Synthesis of S-1-Dodecyl-S′-(*α,α′*-dimethyl-*α″*-acetic acid)-trithiocarbonate (DDMAT) [52]

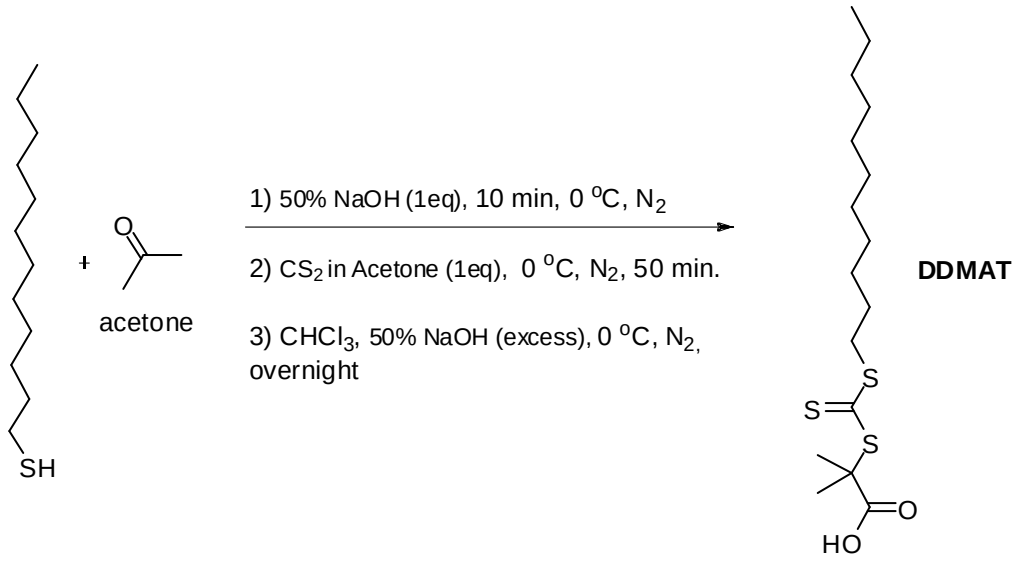

A stirred solution of 1-dodecanethiol (20.2 g, 0.10 mol), and tricaprylylmethylammonium chloride (1.0 g, 0.0025 mol) in acetone (58.0 g, 1.0 mol) at 0 °C under a nitrogen atmosphere, sodium hydroxide (50%) (8.4 g, 0.11 mol) was added over 10 min to the solution. The resulting solution was stirred for an additional 20 min. carbon disulfide (7.6 g, 0.10 mol) in acetone (10.0 g) was added over 30 min, and the color gradually turned red. After chloroform (18 g, 0.15 mol) was added, 50% aqueous sodium hydroxide (40 g) was added dropwise over 20 min. The mixture was stirred overnight. Water (200 mL) was added, followed by 80 mL of concentrated HCl to acidify the aqueous solution. After removing acetone, the solid was collected, and then stirred in 300 mL of 2-propanol. The undissolved solid was filtered off. The

2-propanol solution was concentrated, and the resulting solid was recrystallized from hexane to afford 9.1 g (25% yield) of the product.

S-1-Dodecyl-S′-(*α,α′*-dimethyl-*α′′*-acetic acid)-trithiocarbonate (DDMAT) :Bright yellow crystals, 25% yield; mp 60-61 ^{o}C, ATR-IR: 2955, 2920, 2851, 1735, 1714, 1485, 1436, 1282, 1083, 1069, 815 cm^{-1}. ^{1}H-NMR (in $CDCl_3$): δ 0.9 (t, 3H), 1.30-1.5 (m, 18H), 1.6-1.8 (m, 8H), 3.3 (t, 2H) ppm.

3.3.2 Synthesis of S-1-Dodecyl-S′-(*α,α′*-dimethyl-*α′′*-methyl acetate)-trithiocarbonate (DDMMAT) [53]

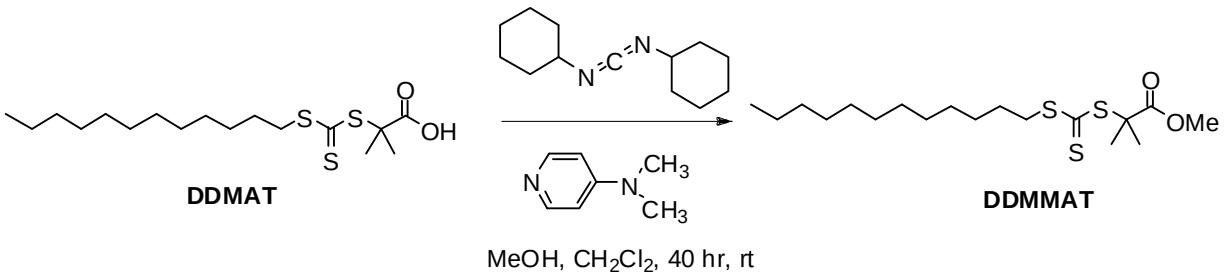

To a stirred solution of DDMAT (2.9 g, 8.0 mmol), CH_3OH (0.7 g, 25 mmol), dicyclohexylcarbodiimide (DCC) (1.7 g, 8.4 mmol) in CH_2Cl_2 (100 mL), 4-dimethylamino- pyridine (DMAP, 0.10 g, 0.80 mmol) were added to the solution. The resulting solution was stirred at room temperature under a nitrogen atmosphere for 40 h. The mixture was filtered, then rotary evaporation gave a yellow oil, which was purified by column chromatography on silica gel, eluting with CH_2Cl_2/hexane (1:4 v/v) to give 2.8 g (91% yield) of the product

S-1-Dodecyl-S′-(*α,α′*-dimethyl-*α′′*-methyl acetate)-trithiocarbonate (DDMMAT): yellow oil, 91% yield, ATR-IR: 2926, , 2906, 2856, 1728, 1723, 1462, 1364, 1261, 1154, 1127, 1068, 816 cm^{-1}. ^{1}H-NMR (in $CDCl_3$): δ 0.9 (t, 3H), 1.30-1.5 (m, 18H), 1.6-1.8 (m, 8H), 3.3 (t, 2H), 3.7 (s, 3H) ppm.

3.4 Synthesis of amphiphilic polymer by RAFT polymerization

3.4.1 Synthesis of poly (N-(2-hydroxyethyl)maleimide-*co*-1-octadecene)

The polymerization procedure is performed as the following procedure: N-(2-hydroxyethyl)maleimide (0.066 g, 0.47 mmol), 1-octadecene (0.12 g, 0.15 ml, 0.47 mmol), DDMAT (2.3 mg, 6.3 µmol) and AIBN (0.21 mg, 1.3 µmol) were added along with drying solvent (2 ml). The mixture was degassed and then sealed under a vacuum. The flask was then immersed into an oil bath to start the polymerization under nitrogen gas. After 24 h, the reaction flask was quenched under atmospheric pressure in icebath to stop the polymerization. Three cycles of precipitation in diethyl ether were perform, then the polymer was dried under vacuum for overnight.

The polymerization will be studied with 2 reaction conditions:
1st reaction condition: polymerization at 70 ^{o}C in THF
2nd reaction condition: polymerization at 90 ^{o}C in 1,4-dioxane

3.4.2 Synthesis of poly(maleic anhydride-*co*-1-octadecene) derivative

3.4.2.1 Synthesis of poly(maleic anhydride-*co*-1-octadecene), PMAO

The polymerization procedure is performed as the following procedure: maleic anhydride (0.98 g, 10 mmol), 1-octadecene (2.6 g, 3.3 ml, 10 mmol), DDMMAT (0.045 g, 0.12 mmol) and AIBN (4.0 mg, 0.024 mmol) were added along with 1,4-Dioxane (5 ml). The flask was then immersed into an oil bath at 90 °C to start the polymerization. After 12 h, the reaction flask was quenched under atmospheric pressure in icebath to stop the polymerization. Three cycles of precipitation in methanol were performed, then the polymer was dried under vacuum for overnight.

3.4.2.2 Synthesis of poly(maleic anhydride-*co*-1-octadecene) derivative

A stirred solution of PMAO (0.2 g) in $CHCl_3$ (2 ml), 10-fold molar excess of 2-(2-aminoethoxy)-ethanol (0.60 g, 0.57 ml, 5.7 mmol) was added to the solution. The resulting solution was stirred at room temperature for overnight then purified with dialysis technique. Then, The resulting polymer was redissolved in buffer pH 7.4 (5 ml). Next, 2-(2-aminoethoxy)-ethanol (0.60 g, 0.57 ml, 5.7 mmol), 1-ethyl-3-(3-dimethylaminopropyl) carbodiimide (EDC) (0.55 g, 2.9 mmol) and *N*-hydroxysulfo succinimide (Sulfo NHS) (5.1 mg, 25µmol) was added to the solution. The resulting solution was stirred at room temperature for overnight then purified with dialysis technique.

Dialysis technique: : sample was put into dialysis bag which have molecular weight cut off as 5000 D. Then, both edges of the bag needed to be tight. The bag, contained sample, was immersed into water bath with a stir at room temperture for a day. Water needed to be changed every 6 h. After 24 h, sample was dried by freeze drying technique.

3.5 Synthesis and characterization of monodispersed magnetite nanoparticles

Monodispersed magnetite nanoparticles were prepared by thermal decomposition of iron carboxylate salts, FeO(OH) [54]. A mixture of FeO(OH) powder and oleic acid and 50 g of 1-octadecene was heated under stirring to 320 ^{o}C for 70 min. This process could provide small and size uniformed magnetite nanoparticles. In addition. the effect of oleic acid to the size of magnetite nanoparticles was performed in this study. Excess oleic acid and unreacted FeOOH were removed by extracting the nanoparticle suspension 3x with a 1:1 (v/v) methanol:chloroform solution. Acetone was then used to precipitate the nanoparticles from the 1-octadecene phase. The morphology of prepared magnetite solutions will be

investigated by TEM. The formula for the production of magnetite nanoparticles will be studied as follows:

Table 3.2 Formula for the production of magnetite nanoparticles

Chemical	**Formula**		
	1	**2**	**3**
1) FeO(OH) (mmol)	10	10	10
2) Oleic acid (mmol)	40	60	80

3.6 Preparation of amphiphilic polymer-coated magnetite dispersion

3.6.1 Preparation of poly(N-(2-hydroxyethyl)maleimide-*co*-1-octadecene)-coated magnetite dispersion

Monodisperse magnetite nanoparticles solution (particle size: 11 nm) (0.1 ml) and poly (N-(2-hydroxyethyl)maleimide-*co*-1-octadecene) solution (polymer (0.3 g) in $CHCl_3$ (2 ml)) were mixed and stirred at room temperature for 12 h. After that, water (2 ml) was slightly added and stirred at room temperature for 12 h. Then, chloroform was then slowly removed by using rotary evaporator.

3.6.2 Preparation of poly(maleic anhydride-*co*-1-octadecene) derivative -coated magnetite dispersion

Monodisperse magnetite nanoparticles solution (particle size: 11 nm) (0.05 ml) and poly(N-(2-hydroxyethyl)maleimide-*co*-1-octadecene) derivative solution (poly(N-(2-hydroxyethyl)maleimide-*co*-1-octadecene) derivative (0.15 g) in $CHCl_3$ (2 ml)) were mixed and stirred at room temperature for 12 h. After that, water (2 ml) was slightly added and stirred at room temperature for 12 h. Then, chloroform was then slowly removed by using rotary evaporator.

CHAPTER IV

RESULTS AND DISCUSSION

The main feature of this research was focused on the production of amphiphilic polymer-coated magnetite dispersion. This chapter could be divided into 4 parts: synthesis of RAFT agents, synthesis of amphiphilic polymers, synthesis of monodispersed magnetite nanoparticles and preparation of well-dispersed amphiphilic polymer-coated magnetite.

4.1 Synthesis and characterization of RAFT agents

RAFT agent plays an important role in controlling the evolution of the molecular weight distribution with the rate of conversion and the rate of polymerization. In this research study, two types of RAFT agents, trithiocarbonate acid and trithiocarbonate methyl ester were synthesized for further polymerization.

4.1.1 Synthesis and characterization of S-1-dodecyl-S′-(*α,α′*-dimethyl-*α′′*-acetic acid)-trithiocarbonate (DDMAT)

DDMAT is a very efficient chain-transfer RAFT agent. This was because the carboxyl-stabilized tertiary carbon radical was employed when the carbon-sulfur single bond is broken during polymerizations as shown in Scheme 4.1.

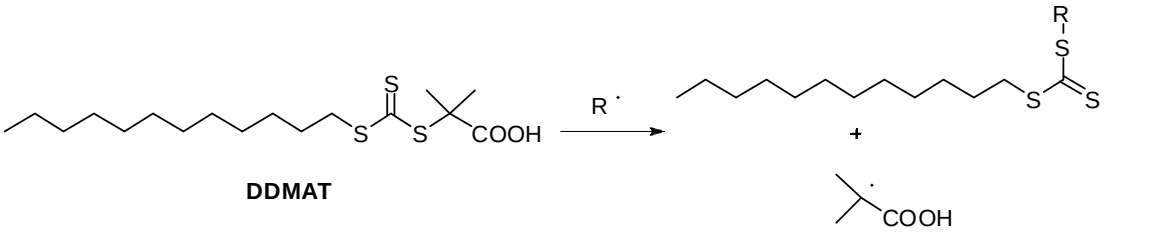

DDMAT

R• radical

Carboxyl-stabilized tertiary carbon radical

Scheme 4.1 Addition and fragmentation reaction of DDMAT

DDMAT was synthesized in one step from 1-dodecanethiol, acetone, carbon disulfide and chloroform following a literature procedure [52]. The product was obtained as yellow crystal, 25 % yield ([52], 65%). According to the experimental experience, it was noticed that one of the important factor to success in the synthesis is the stirring rate of the reaction. Many failures of the synthesis were met when a conventional magnetic stirrer was attempted. It was recommended to stir vigorously during the reaction process in order to get the productive yield of DDMAT. The characterization of DDMAT was obtained by ATR-IR and ^{1}H-NMR spectroscopy. As for ATR-IR spectra in Table 4.1 and Figure 4.1, all characteristic peaks of the product were observed, for example, absorption bands at 1714 and 1083 cm^{-1}, corresponding to C=O stretching of carboxylic acid and S-C stretching of thiocarbonate, respectively. ^{1}H-NMR data also affirmed the structure of the DDMAT as described in Table 4.2 and Figure 4.2

Table 4.1 ATR- IR absorption band assignment of DDMAT

Wave number (cm^{-1})	**Intensity**	**Vibration**
3300-2500	Broad	O-H stretching vibration of carboxylic acid
2955, 2920, 2851	Weak, medium, medium	C-H stretching vibration of aliphatic hydrocarbon
1714	Strong	C=O stretching vibration
1083	Medium	C-S stretching vibration
1070	Medium	C-O stretching vibration

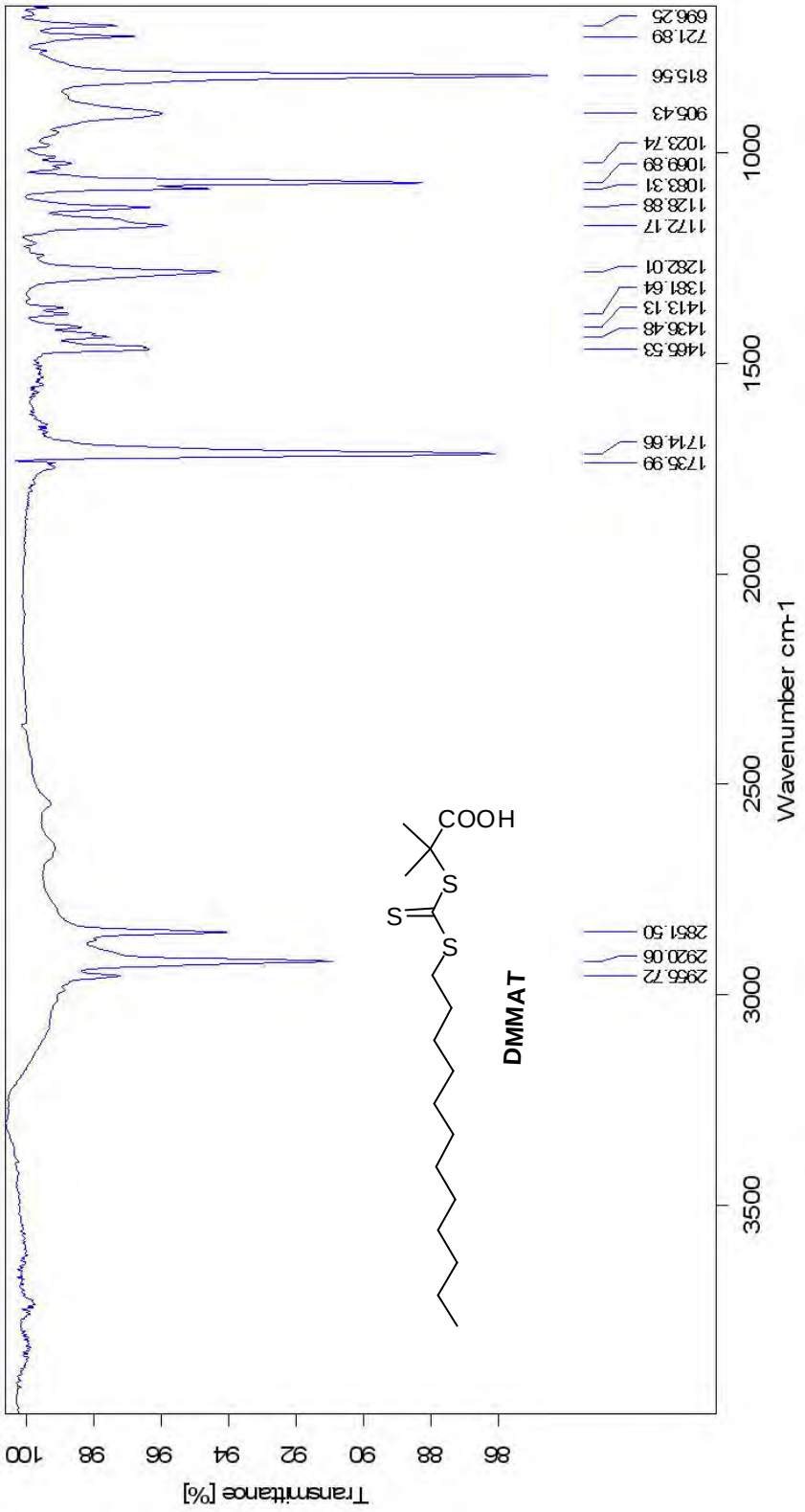

Figure 4.1 ATR-IR spectra of DDMAT

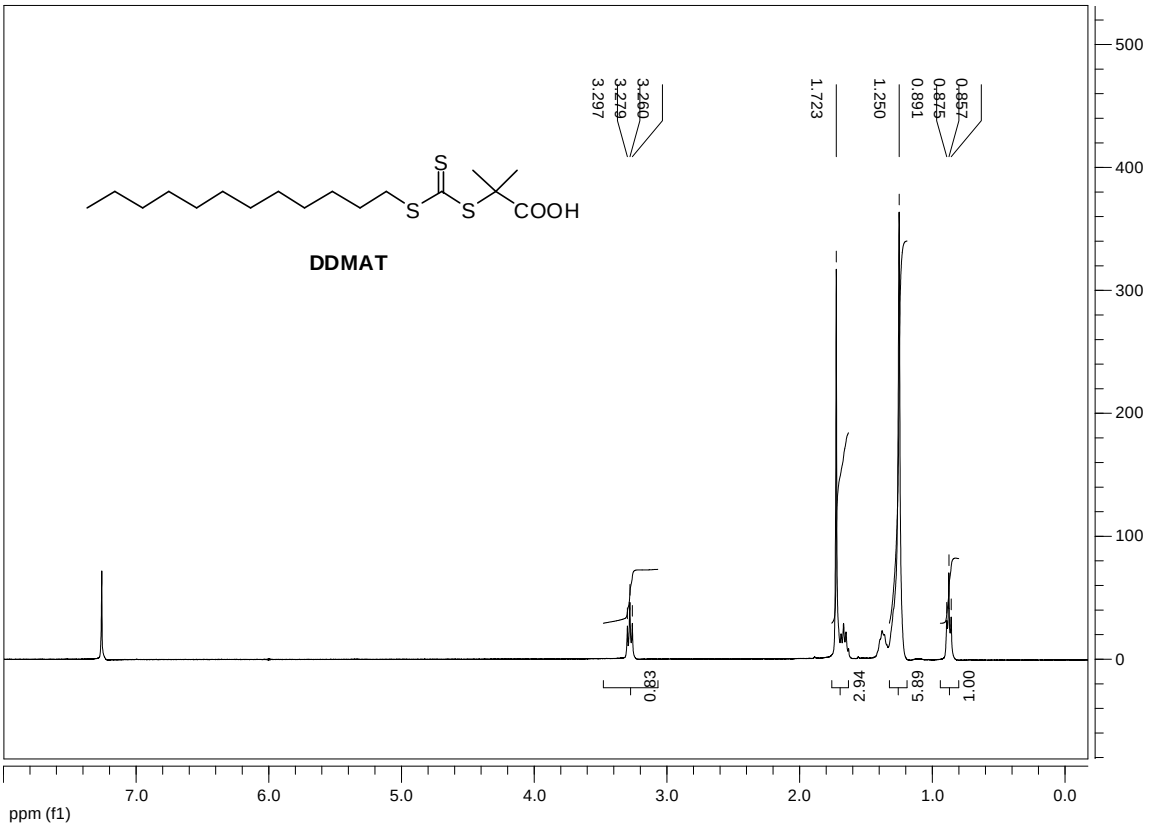

Figure 4.2 ^{1}H-NMR spectrum of DDMAT

Table 4.2 ^{1}H-NMR data assignment of DDMAT

Chemical Shift (ppm)	Multiplicity	No. of proton	Details
0.9	triplet	3	$CH_2C\underline{H}_3$
1.3	multiplet	16	-C$\underline{H}_2$-
1.7	multiplet	8	-SCH(C$\underline{H}_3$)$_2$, -C$\underline{H}_2$CH$_2$S-
3.3	triplet	2	-C$\underline{H}_2$S-

In addition, all ATR and ^{1}H-NMR of product complied with the literature reference [52]. From this point the characterization data described above demonstrate that the synthesis of DDMAT was accomplished.

4.1.2 Synthesis and Characterization of S-1-Dodecyl-S′-(*α*,*α*′-dimethyl-*α*′′-methyl acetate)-trithiocarbonate (DDMMAT)

Due to the carboxyl-stabilized tertiary carbon radical similarly to DDMAT structure, DDMMAT was also mentioned as the high efficient chain-transfer RAFT agents. The methyl ester of trithiocarbonate was designed for the purpose of protecting group of carboxylic acid. After RAFT polymerization, the telechelic polymer can be deprotected the ester functional group which would generate the free carboxylic acid for any further application.

DDMMAT was synthesized in one step from DDMAT, methanol and dicyclohexylcarbodiimide in accordance with a literature procedure [53]. The product was obtained as yellow oil, 91% yield ([53], 94%). As for ATR-IR data in Table 4.3 and Figure 4.3, all characteristic peaks of the product were observed, for example, C=O stretching of ester and S-C stretching of trithiocarbonate at 1739 and 1154 cm^{-1}, respectively. The ^{1}H-NMR data confirmed the success of the DDMMAT synthesis as shown in Table 4.4 and Figure 4.4, especially singlet peak of methyl proton of carboxylate ester δ 3.7 ppm, confirming the existing of methyl ester. In addition, the resulting ATR-IR and ^{1}H-NMR of product were both complied with the literature reference [53].

Table 4.3 ATR- IR absorption band assignment of DDMMAT

Wave number (cm^{-1})	Intensity	Vibration
3300-2500	broad	O-H stretching vibration of hydroxyl group
2926, 2906, 2856	medium, weak, weak	C-H stretching vibration
1739	strong	C=O stretching vibration
1154	Medium	C-S stretching vibration
1068	Medium	C-O stretching vibration

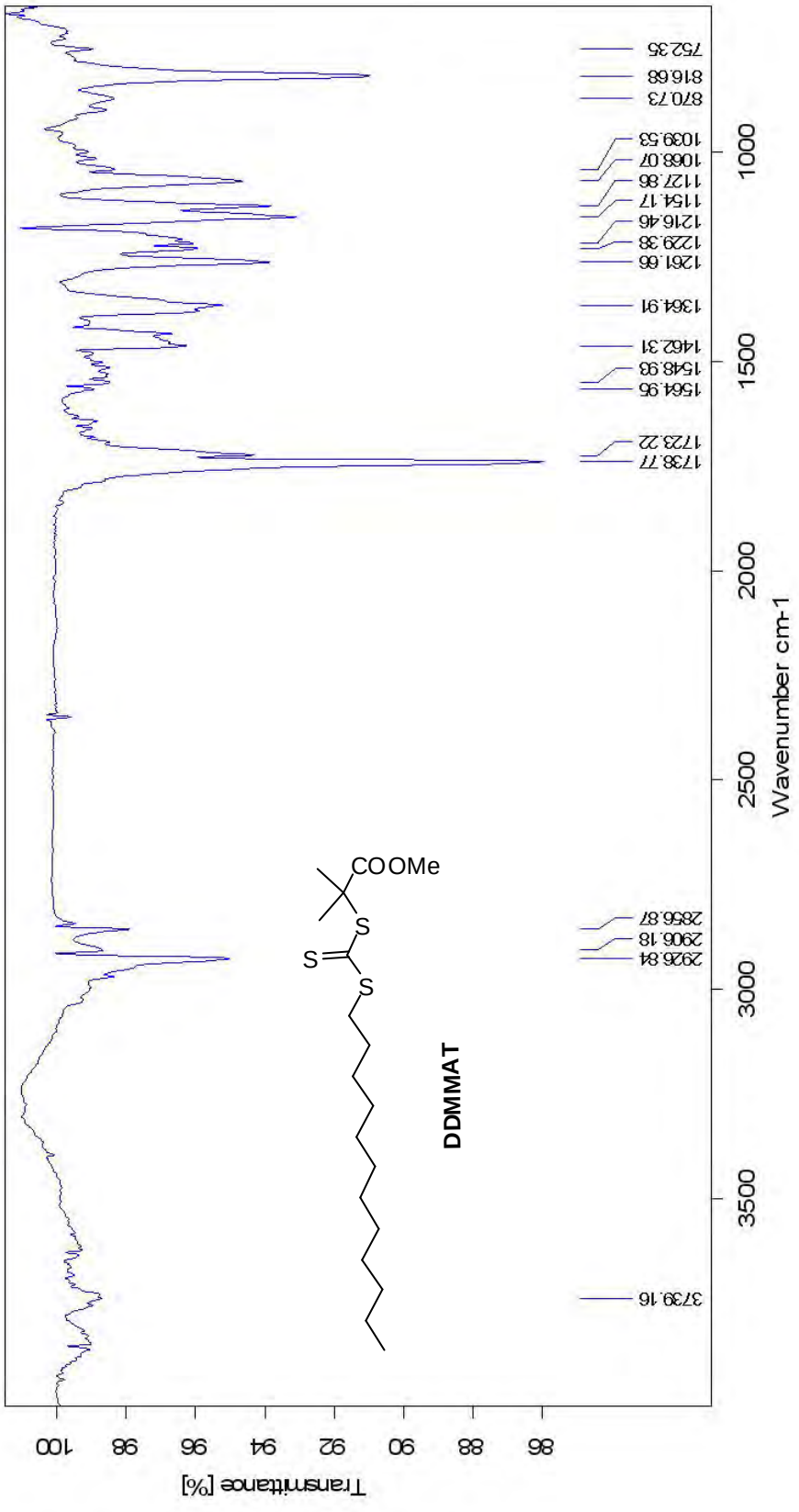

Figure 4.3 ATR-IR spectra of DDMMAT

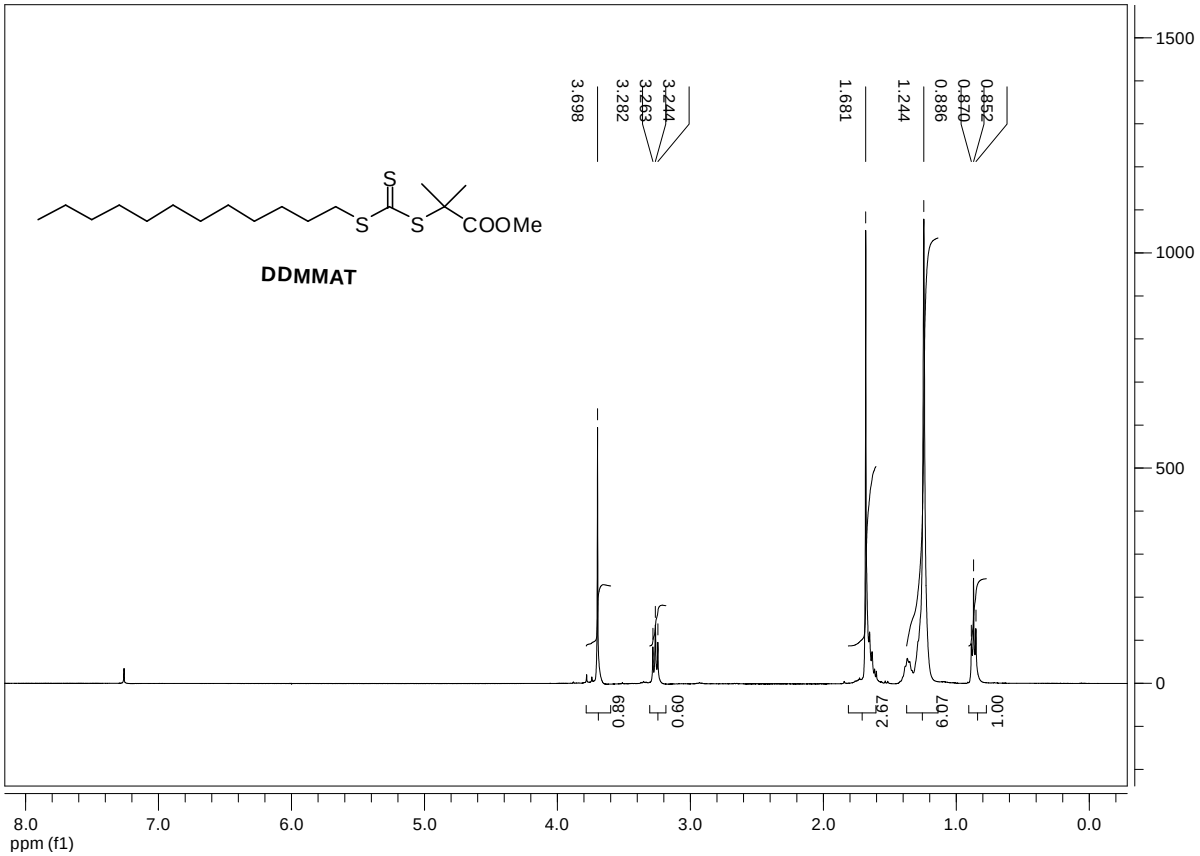

Figure 4.4 ^{1}H-NMR spectrum of DDMMAT

Table 4.4 ^{1}H-NMR data assignment of DDMMAT

Chemical Shift (ppm)	Multiplicity	No. of proton	Details
0.9	triplet	3	$CH_2C\underline{H}_3$
1.3	multiplet	16	-$C\underline{H}_2$-
1.7	multiplet	8	-$SCH(C\underline{H}_3)_2$, -$C\underline{H}_2CH_2S$-
3.3	triplet	2	-$C\underline{H}_2S$-
3.7	singlet	3	-$OC\underline{H}_3$

4.1.3 Mechanism for DDMAT formation

As for the mechanism for DDMAT formation in Scheme 4.2, the reaction of chloroform (**1**) and OH^- produced highly reactive carbene intermediate **2** which would further react to acetone, giving the intermediate **3**. The abstraction of hydrogen on thiol compound **4**, by hydroxide ion would generate the reactive specie **5** which would further react to acetone, forming trithiocarbonate intermediate **6**. Then, the ring opening of the intermediate **3,** by the approach of the intermediate **6**, would produce the intermediate **7**. The rearrangement of the intermediate **7** would afford acid chloride intermediate **8**. Finally, the approach of OH^- to the intermediate **8** created DDMAT **(9)**.

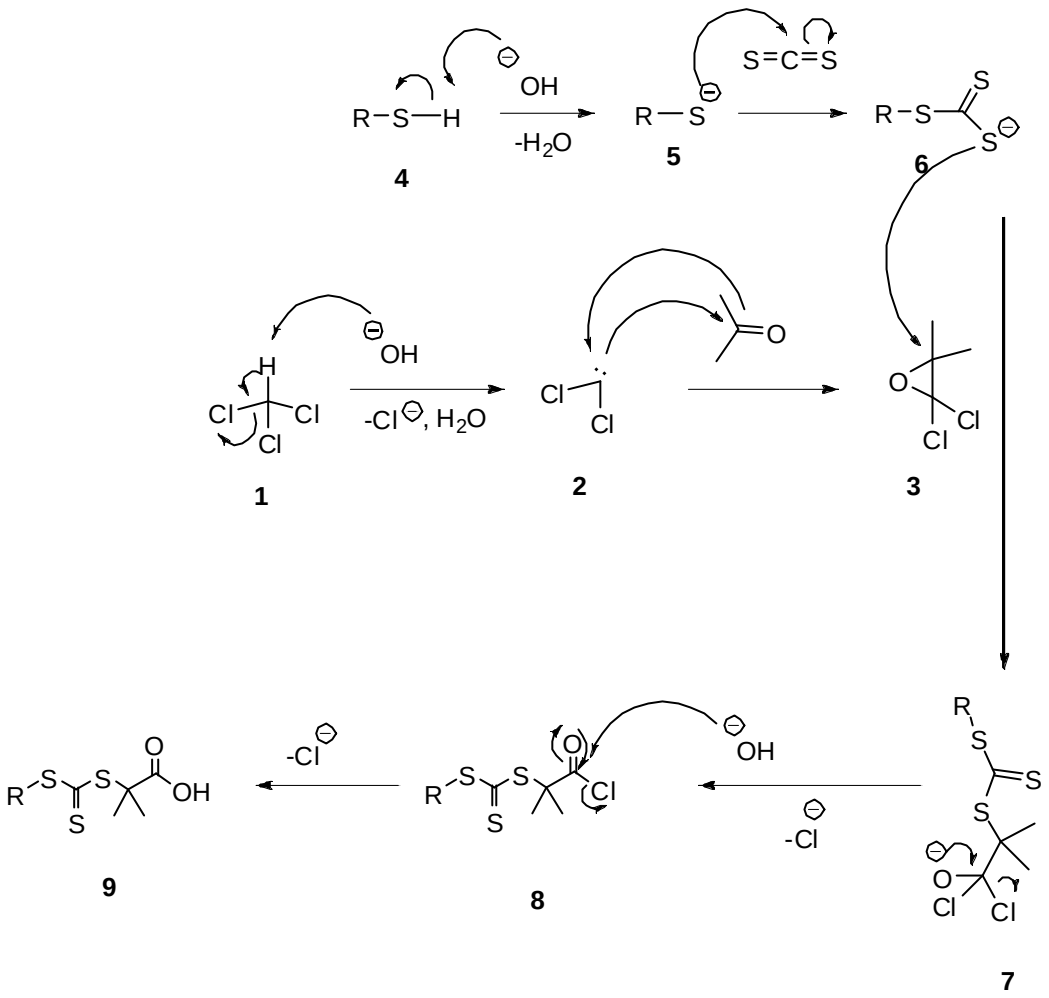

Scheme 4.2 Mechanism for DDMAT formation

4.1.3 Mechanism for DDMMAT formation

Regarding to the mechanism for DDMMAT formation in Scheme 4.3, The acid **10** would react with the carbodiimide **11** to produce intermediate **12** and **13**. The reaction of intermediate **12** and **13** will be provided the key intermediate, O-acylisourea **(14)**, that could be viewed as a carboxylic ester with an activated leaving group. The O-acylisourea would react with DMAP to give the intermediate **16** and urea. Then, methoxide ion would react with intermediate 16 to produce DDMMAT as the final product.

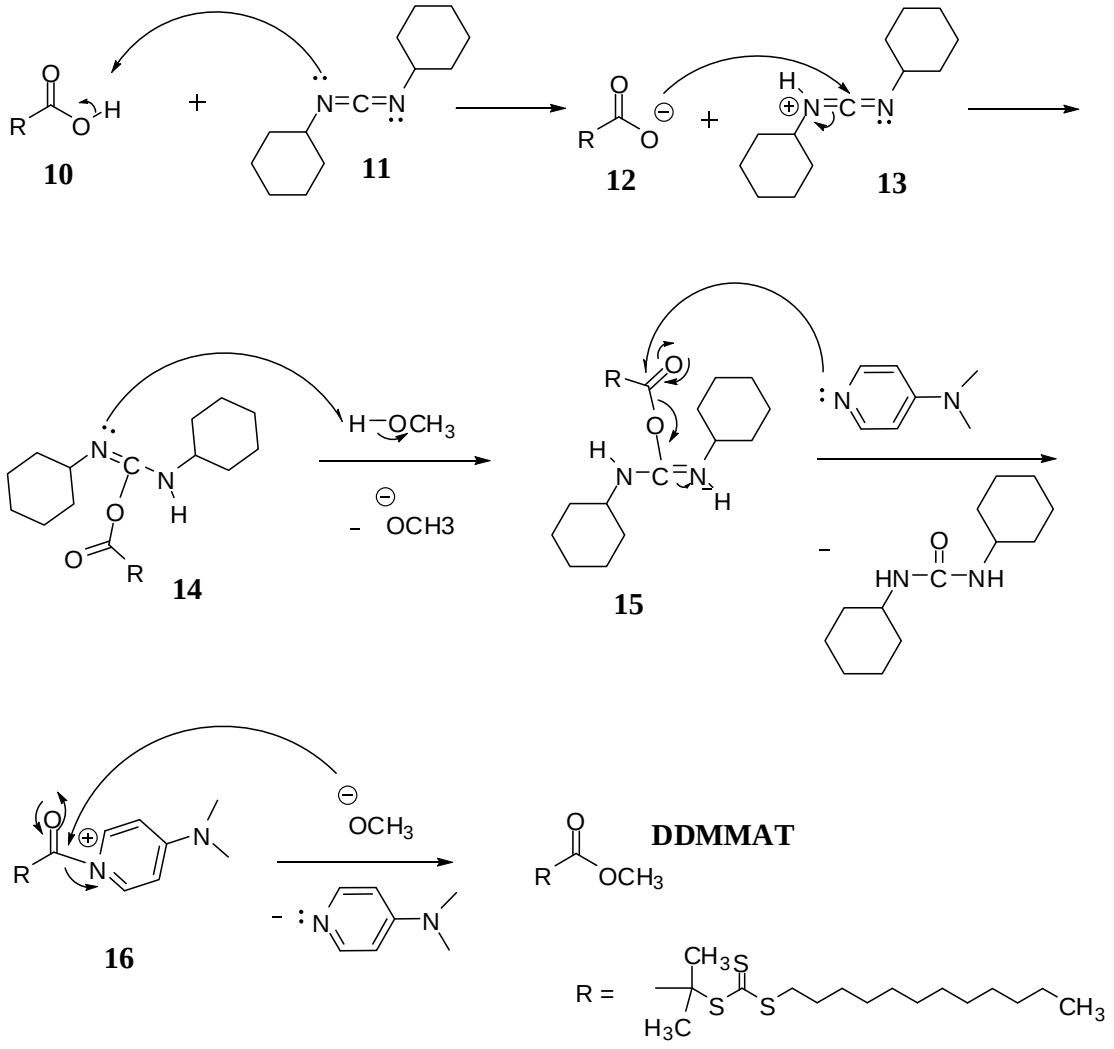

Scheme 4.3 Mechanism for DDMMAT formation

4.2 Synthesis of amphiphilic polymers by RAFT polymerization

With the importance of amphiphilic copolymers and their ability to afford well-defined material, the use of amphiphilic copolymers for the construction of functional magnetite nanoparticles has been interested. Two kind of amphiphilic copolymers, hydrophobic aliphatic hydrocarbon and hydrophilic ethylene glycol, were synthesized by RAFT polymerization. The polymer was designed to use ethylene glycol units as hydrophilic site due to its excellent biocompatibility whereas hydrophobic aliphatic hydrocarbon can hypothetically adsorb onto the pre-synthesized magnetite nanoparticles coated with oleic acid primary surfactant.

4.2.1 Synthesis and Characterization of poly(N-(2-hydroxyethyl)maleimide-*co*-1-octadecene)

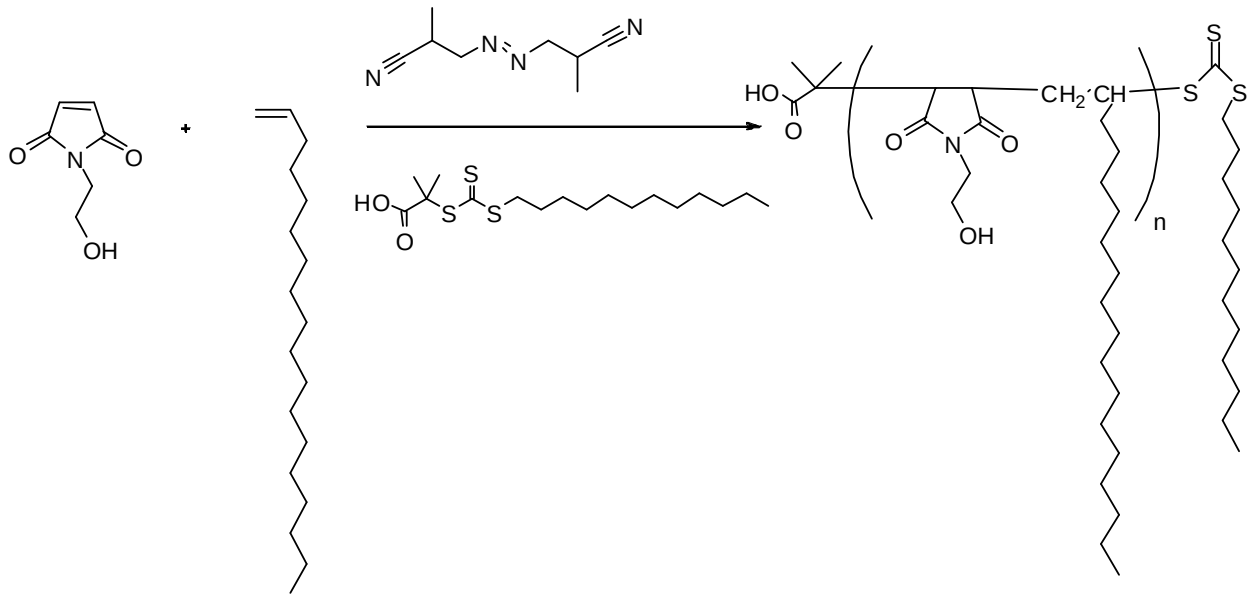

RAFT copolymerization of N-(2-hydroxyethyl)maleimide and 1-octadecene ([N-(2-hydroxyethyl)maleimide]/[1-octadecene]/[AIBN]/[DMMAT] 85:85:0.2:1) was conducted into two reaction condition, 70 ^{o}C in THF and 90 ^{o}C in 1,4-dioxane. The polymerization was allowed to proceed for 24 h. The copolymer was obtained as

white solid after precipitation with diethyl ether three times and carried out molecular weight by GPC technique. The resulting GPC was demonstrated in Figure 4.5 and 4.6.

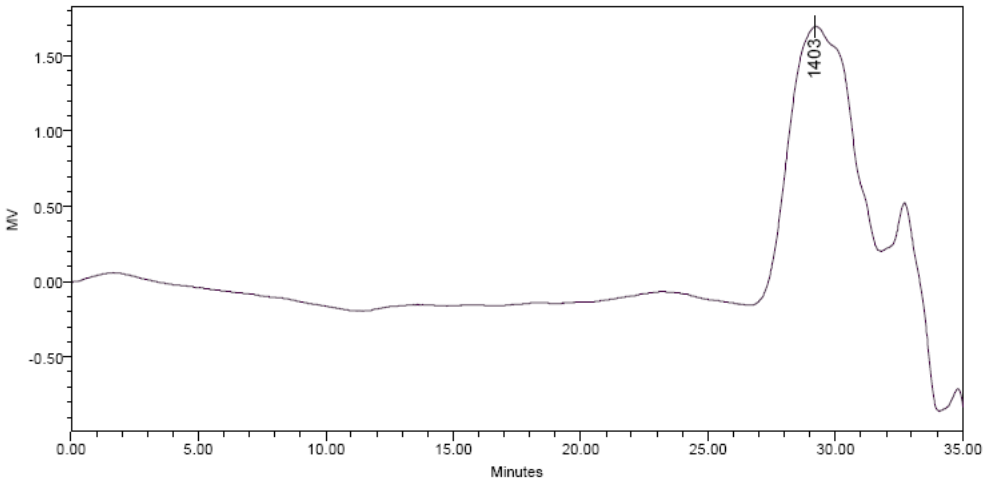

Figure 4.5 GPC chromatogram of poly(N-(2-hydroxyethyl)maleimide-*co*-1-octadecene)

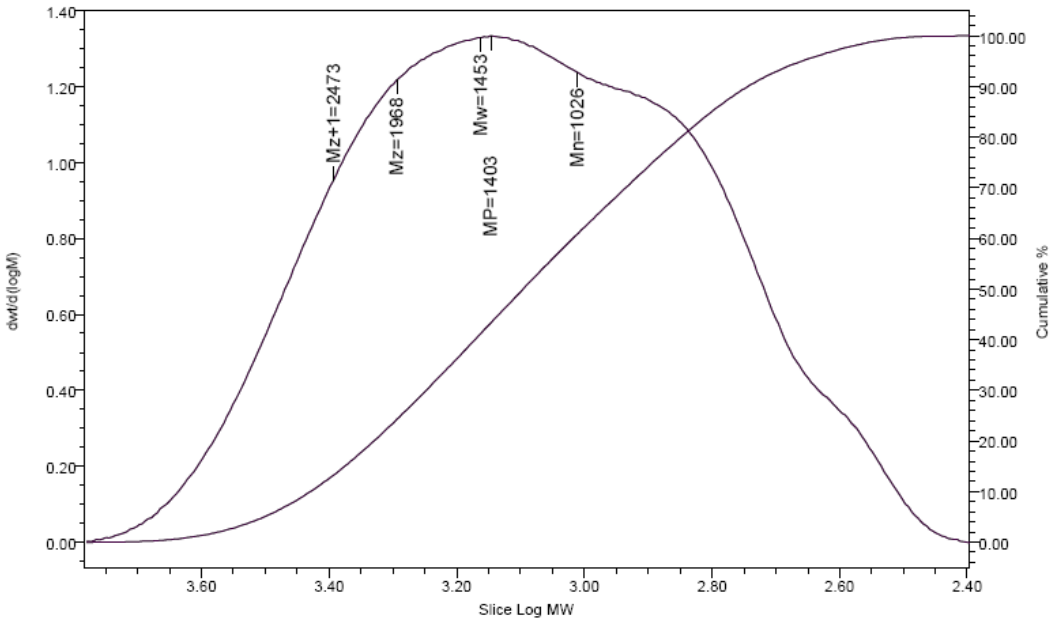

Figure 4.6 Standard PS calibration curve and molar mass distribution of poly(N-(2-hydroxyethyl)maleimide-*co*-1-octadecene)

Table 4.5 GPC result of poly(N-(2-hydroxyethyl)maleimide-*co*-1-octadecene)

No.	Condition	M_w	M_n	PDI
1	70°C, THF	1453	1026	1.42
2	90°C, 1,4-dioxane	1199	868	1.38

Regarding to the result in Table 4.5, there is no significant different of Mw, Mn and PDI of poly(N-(2-hydroxyethyl)maleimide-*co*-1-octadecene) when studying conditions was various. Mn and Mw of copolymer which performed at 70°C in THF were slightly higher than the polymerization at 90°C in dioxane. In addition, the number average molecular weight of the copolymer was smaller than molecular weight from theoretical calculation which was expected to get as 30000 D. This might be caused by chain transfer reaction of polymer and N-(2-hydroxyethyl)maleimide as shown in Figure 4.7

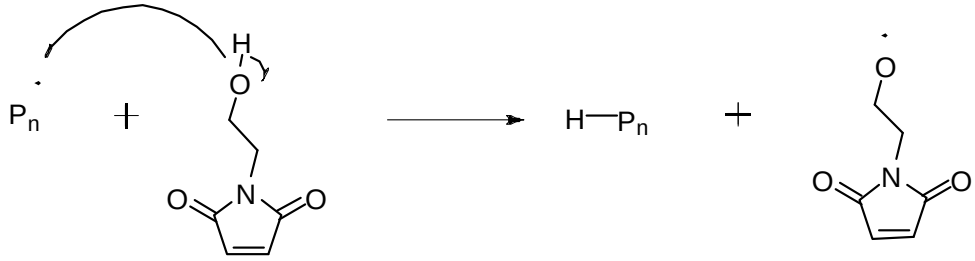

Figure 4.7 Chain transfer reaction of polymer and N-(2-hydroxyethyl)maleimide

The copolymer was characterized by ATR-IR, GPC and ^{1}H-NMR. In Figure 4.8 and Table 4.6, it revealed characteristic absorption spectra of poly(N-(2-hydroxyethyl)maleimide-*co*-1-octadecene) at 1772 and 1683 cm^{-1} which attributed to C=O stretching of amide. The ^{1}H-NMR spectra in Figure 4.9 and Table 4.7 revealed methylene protons, which connected to oxygen atom, of ethylene glycol unit at δ 3.6 ppm as a broad peak and methylene and methyl protons of aliphatic hydrocarbon of 1-octadecene unit at δ 0.8 and 1.2 ppm, respectively. The characterization data described above indicated that the synthesis of poly(N-(2-hydroxyethyl)- maleimide-*co*-1-octadecene) was accomplished.

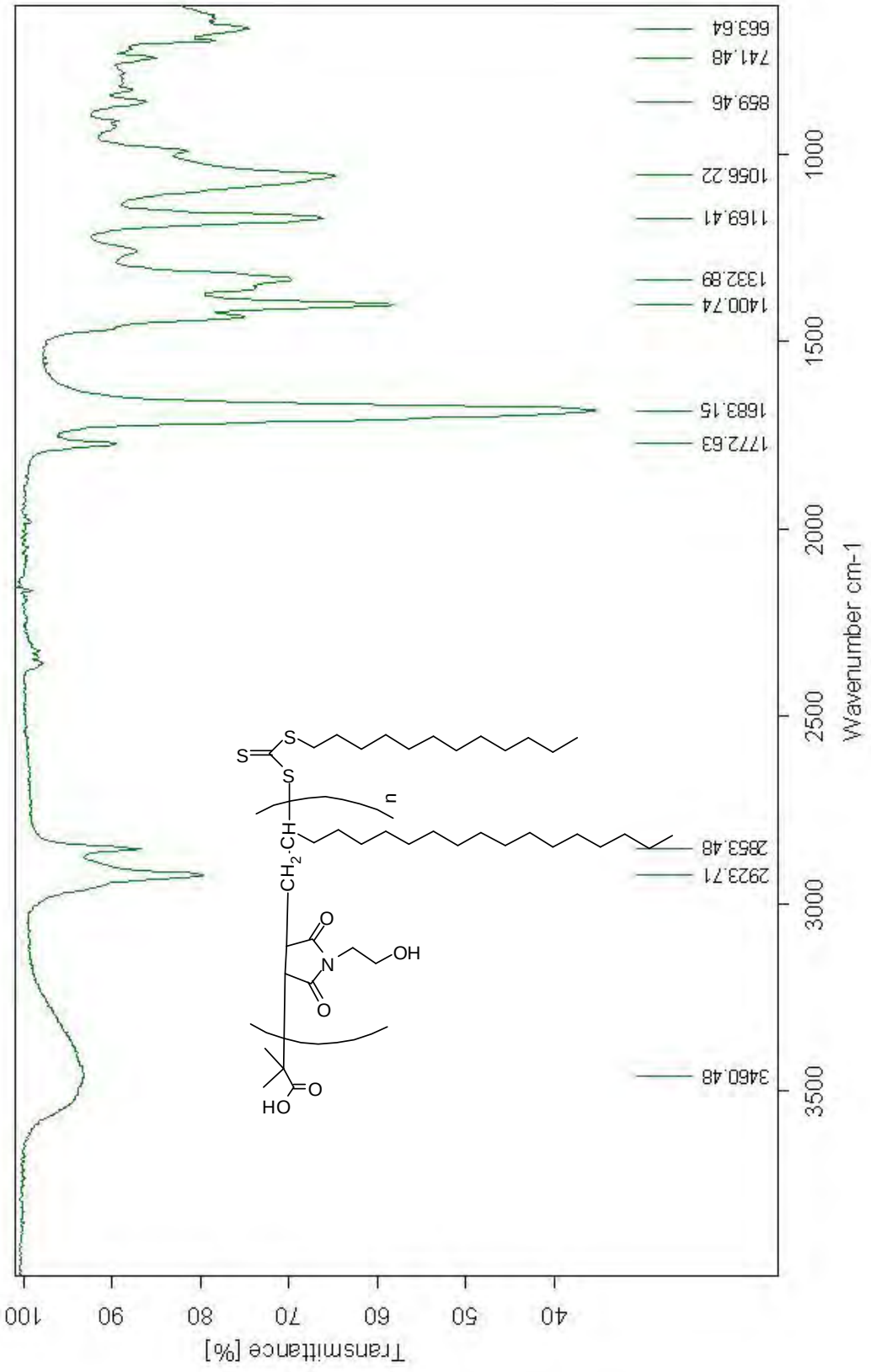

Figure 4.8 ATR-IR spectra of poly (N-(2-hydroxyethyl) maleimide-*co*-1-octadecene)

Table 4.6 ATR-IR absorption band assignment of poly(N-(2- hydroxyethyl)-maleimide-*co*-1-octadecene)

Wave number (cm^{-1})	Intensity	Vibration
2926, 2856	Medium, medium	C-H stretching vibration of hydrocarbon
1772, 1683	Weak, strong	C=O stretching vibration of tertially amide
1169	Medium	C-N stretching vibration
1056	Medium	C-O stretching vibration

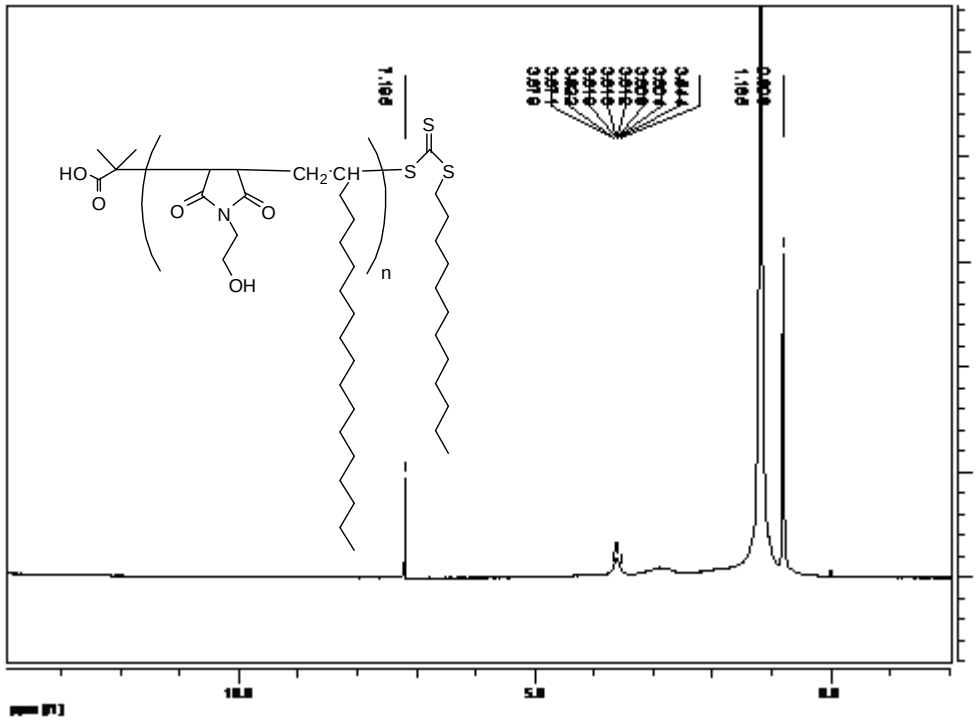

Figure 4.9 ^{1}H-NMR spectrum of poly(N-(2-hydroxyethyl)maleimide-*co*-1-octadecene)

Table 4.7 ^{1}H-NMR data assignment of poly(N-(2-hydroxyethyl)maleimide-*co*-1-octadecene)

Chemical Shift (ppm)	Multiplicity	Details
0.8	multiplet	-$CH_2C\underline{H}_3$
1.2	multiplet	-$C\underline{H}_2$-
3.6	multiplet	-$CH_2C\underline{H}_2O$-

4.2.2 Synthesis and Characterization of poly(maleic anhydride-*co*-1-octadecene) derivative

4.2.2.1 Synthesis and Characterization of poly(maleic anhydride-*co*-1-octadecene) PMAO

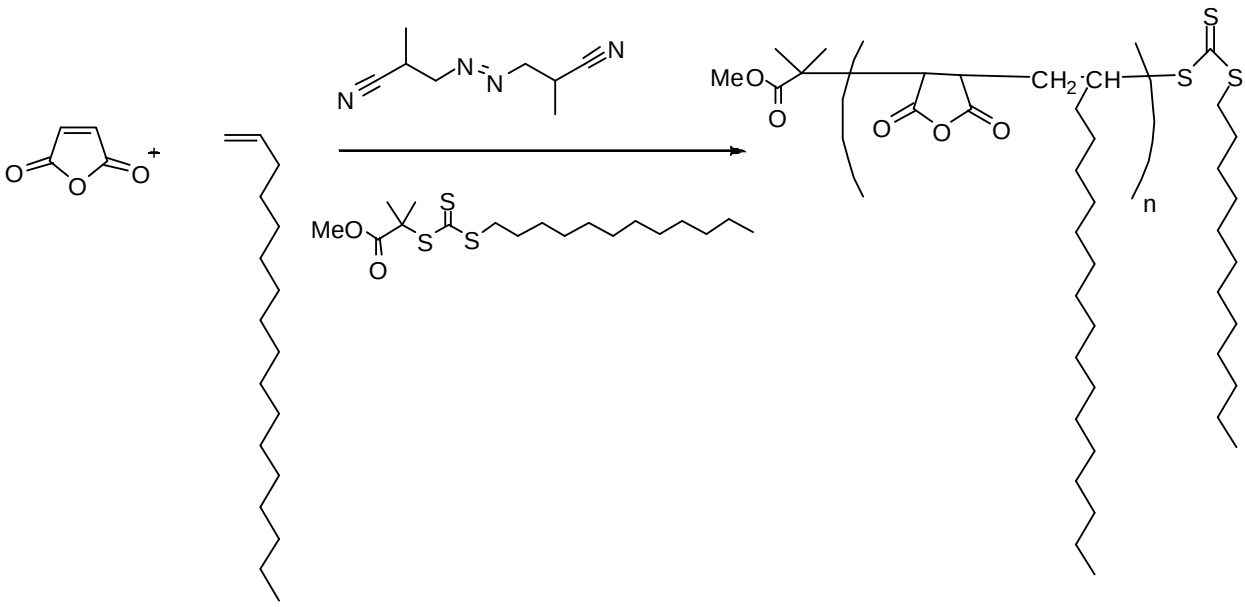

Poly(maleic anhydride-*co*-1-octadecene) was polymerized by RAFT technique. The copolymerization of maleic anhydride and 1-octadecene ([maleic anhydride], [1-octadecene], [AIBN], [DDMMAT] 85:85:0.2:1) was conducted at 90 ^{o}C in 1,4-dioxane for 12 h. After the reaction was finished, the copolymer was purified by precipitation with methanol and obtained as yellow solid.

Then, the resulting product was dried out and analyzed the molecular weight by GPC as shown in Figure 4.10 and 4.11. In Table 4.8, it was affirmed the number average molecular weight of the copolymer as 11,870 D with polydispersity index (PDI) about 1.77, resulting the narrow molecular weight distribution. In addition, the number average molecular weight Mn of the copolymer was smaller than molecular weight from theoretical calculation which was expected to be as 30,000 D.

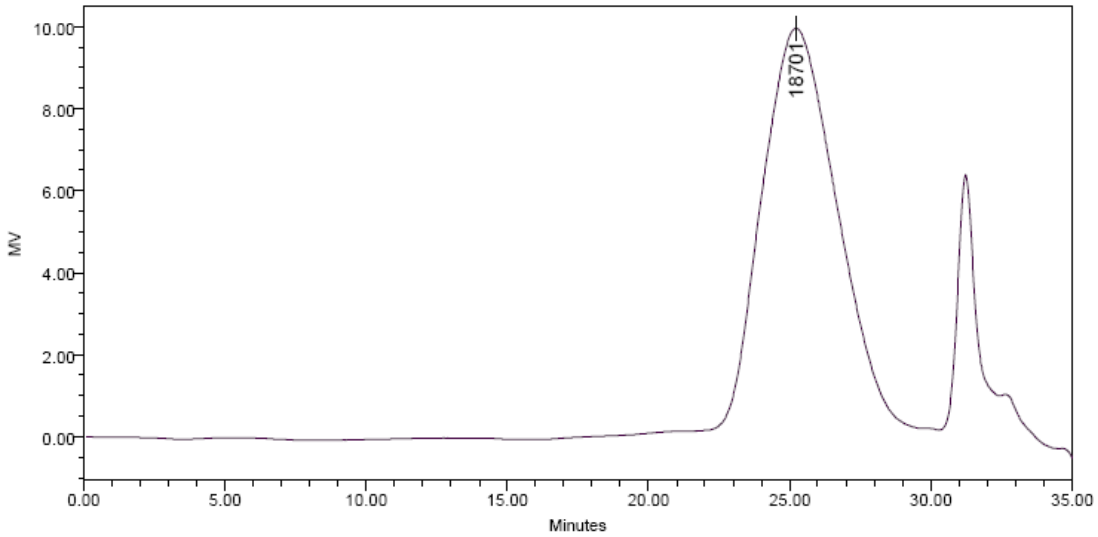

Figure 4.10 GPC chromatogram of poly(maleic anhydride-*co*-1-octadecene)

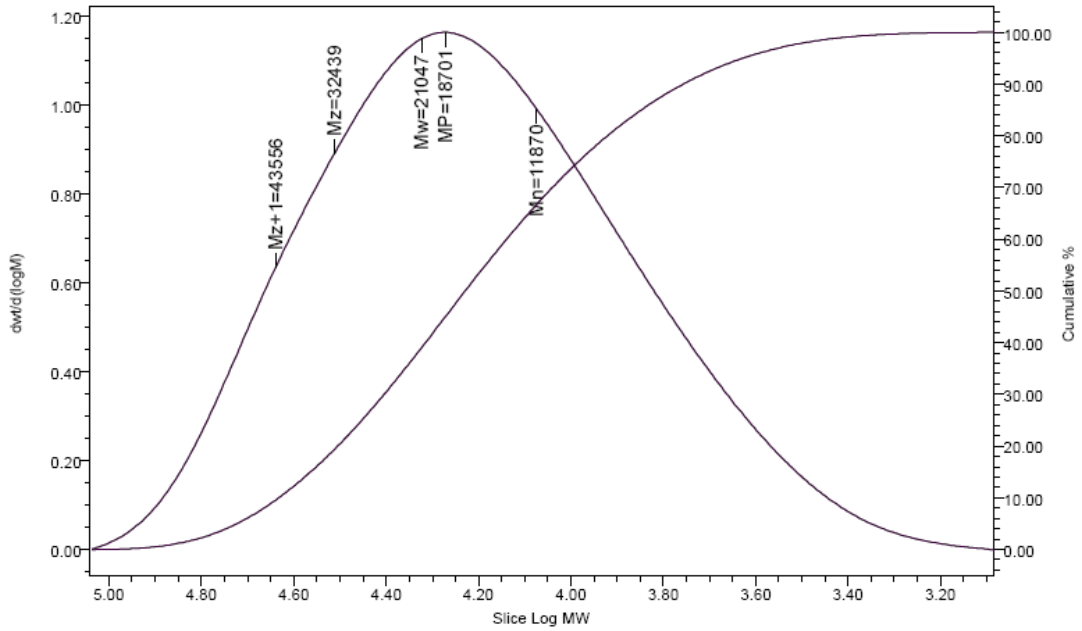

Figure 4.11 Standard PS calibration curve and molar mass distribution of poly(maleic anhydride-*co*-1-octadecene)

Table 4.8 GPC result of of poly(maleic anhydride-*co*-1-octadecene)

Copolymer	M_w	M_n	PDI
poly(maleic anhydride-*co*-1-octadecene)	21047	11870	1.77

The copolymer was characterized by TGA, ATR-FTIR and ^{1}H-NMR. In Figure 4.12, 4.13 and Table 4.19, the thermal composition of PMAO by TGA exhibited three steps of weight loss in the range of 80-1,000 ^oC. The first onset decomposition temperature was measured to be at 150 ^oC with no weight loss in this temperature. At 361 ^oC, the second onset decomposition temperature revealed with a 12% weight loss. This weight loss may involve the elimination of H_2O and CO_2, with the latter at the result of thermal decarboxylation of acid moiety. In addition, the elimination of hexadecane side-chains was performed at high temperatures above 450 ^oC. The thrid onset decomposition temperature was observed at 767 ^oC with a 85% wight loss. In addition, a 50% weight loss of PMAO was measure at 430 ^oC.

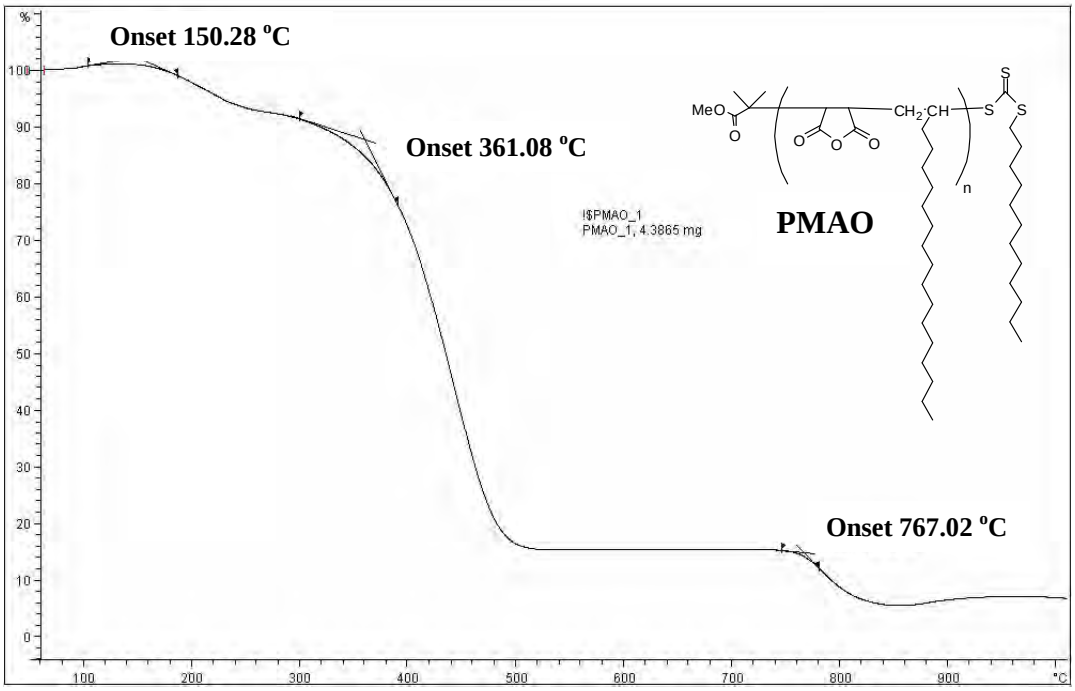

Figure 4.12 Thermogravimetric curve of poly(maleic anhydride-*co*-1-octadecene)

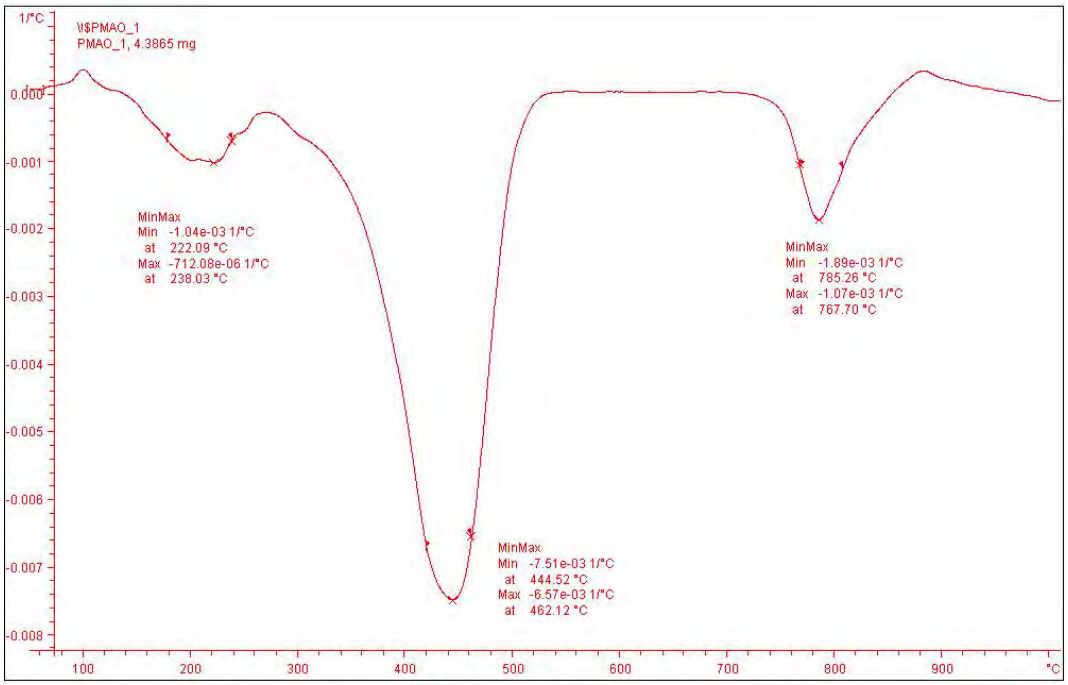

Figure 4.13 Differential thermal analysis curve of poly(maleic anhydride-*co*-1-octadecene)

Table 4.9 Temperature and % weight loss of poly(maleic anhydride-*co*-1-octadecene) by TGA

Temperature (^{o}C)	**% Weight loss**
150	0
240	6
361	12
430	50
500	85
767	85
840	94

Figure 4.14 and Table 4.10 exhibited the ATR-IR data of poly(maleic anhydride-*co*-1-octadecene). Two absorption bands at 1779 and 1746 cm^{-1} contributed to C=O stretching of anhydride and absorption bands at 2908 and 2856 cm^{-1}

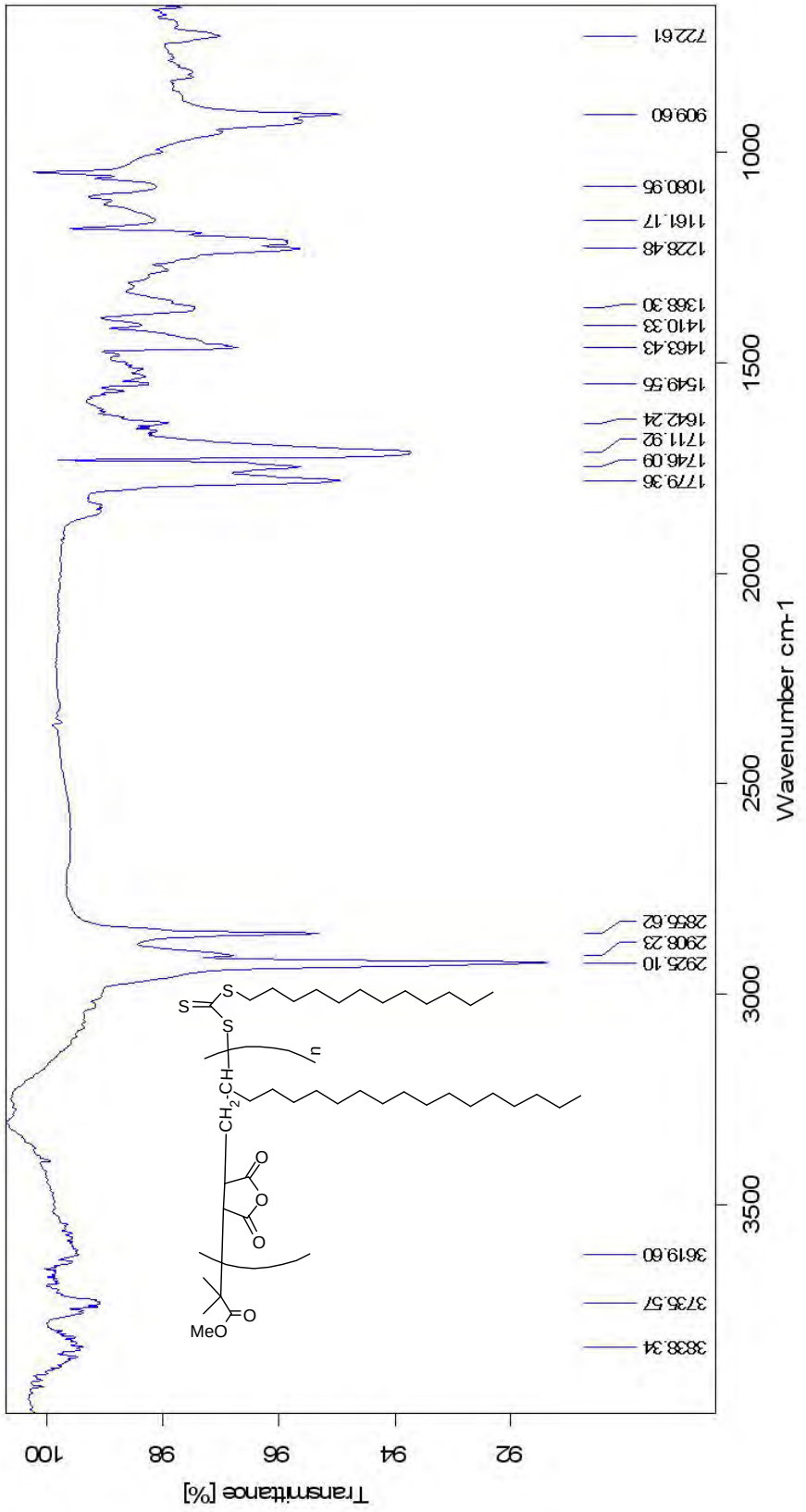

Figure 4.14 ATR-FTIR spectra of poly(maleic anhydride-*co*-1-octadecene)

attributed to C-H stretching of methyl and methylene protons, respectively. As for ^{1}H-NMR spectra of poly(maleic anhydride-*co*-1-octadecene) in Figure 4.7, the signal at δ 0.8 and 1.3 ppm were due to the methyl and methylene proton of poly(maleic anhydride-*co*-1-octadecene).

Table 4.10 ATR-IR absorption band assignment of poly(maleic anhydride-*co*-1-octadecene)

Wave number (cm^{-1})	**Intensity**	**Vibration**
2925, 2908, 2856	strong, medium, medium	C-H stretching vibration
1779, 1746	strong, strong	C=O stretching vibration of anhydride
1228, 909	medium, medium	C-O stretching vibration of anhydride

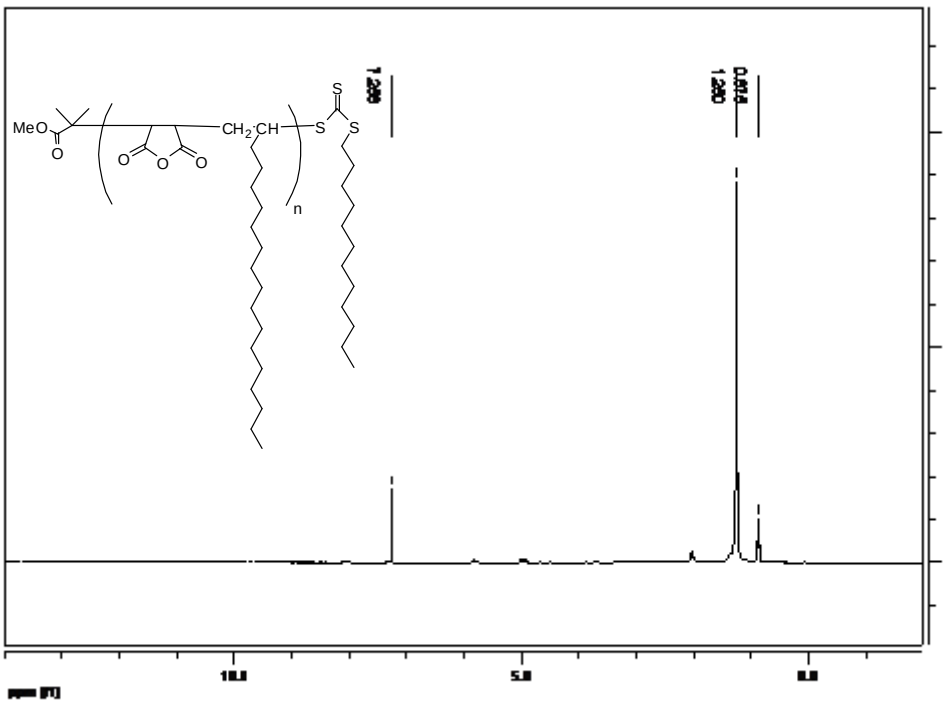

Figure 4.15 ^{1}H-NMR spectrum of poly(maleic anhydride-*co*-1-octadecene)

Table 4.11 ^{1}H-NMR data assignment of poly(maleic anhydride-*co*-1-octadecene)

Chemical Shift (ppm)	Multiplicity	Details
0.8	multiplet	$CH_2C\underline{H}_3$
1.2	multiplet	$-C\underline{H}_2-$

4.2.2.2 Synthesis and Characterization of poly(maleic anhydride-*co*-1-octadecene) derivative

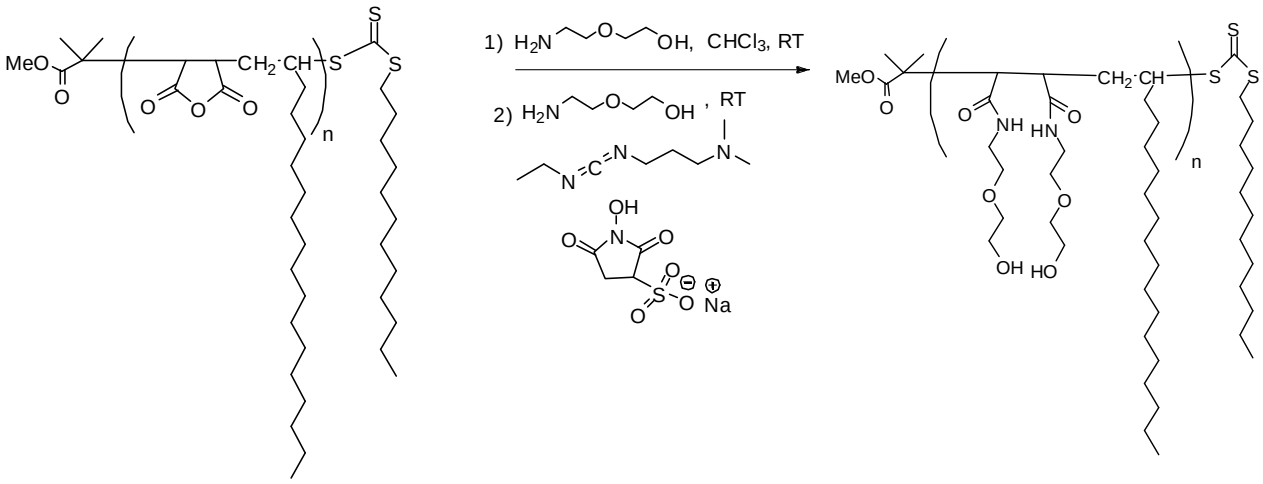

In order to improve the hydrophilicity of poly(maleic anhydride-*co*-1-octadecene), it was required to modify the copolymer to have more additional ethylene glycol unit. Poly(maleic anhydride-*co*-1-octadecene) derivative was prepared as described in Scheme 4.4. Firstly, the ring opening of maleic anhydride by 2-(2-aminoethoxy)-ethanol was carried out, generating free carboxylic and ethylene glycol side chains. Secondly, 2-(2-aminoethoxy)-ethanol was reacted to free carboxylic acid *via* coupling agent, 1-ethyl-3-(3-dimethylaminopropyl) carbodiimide, resulting another glycol side chains. In addition, sulfo-NHS played its role as same as DMAP in Section 4.1.3.

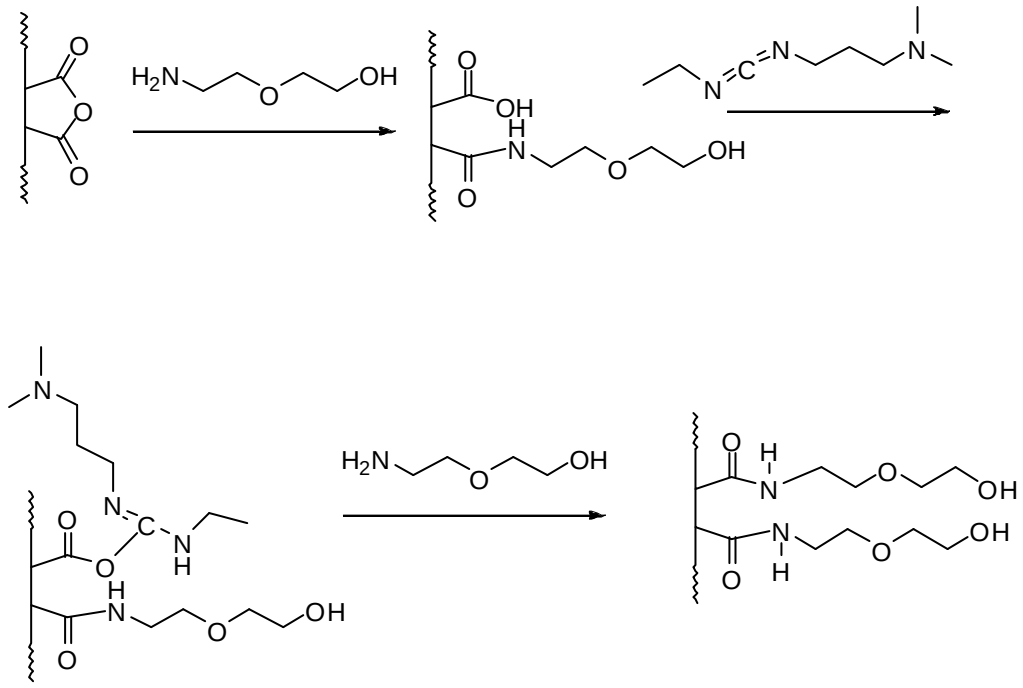

Scheme 4.5 Synthetic routes for the formation of poly(maleic anhydride-*co*-1-octadecene) derivative

The characterization of the synthesized poly(maleic anhydride-*co*-1-octadecene) derivative was accomplished by ATR-FTIR, and ^{1}H-NMR. Regarding to ATR-IR data in Figure 4.16 and Table 4.12, an important absorption band at 1737 cm^{-1} corresponding to C=O stretching of amide was observed, affirming the result of new amide bond form. For ^{1}H-NMR spectra in Figure 4.17 and Table 4.13, it was appeared methylene protons, connected to oxygen atom of ethylene glycol unit at δ 3.6 ppm and methylene and methyl proton of long chain aliphatic hydrocarbon at δ 0.8 and 1.2, respectively. ^{13}C-NMR spectra in Figure 4.18 and Table 4.14 revealed the characteristic peaks of poly(maleic anhydride-*co*-1-octadecene) derivative, especially an important peak at 176 ppm, attributing to C=O of amide bond and peak at 157 ppm, affirming to C=S of amide bond. From these reasons, the characterization data described above indicated that the synthesis of poly(maleic anhydride-*co*-1-octadecene) derivative was accomplished.

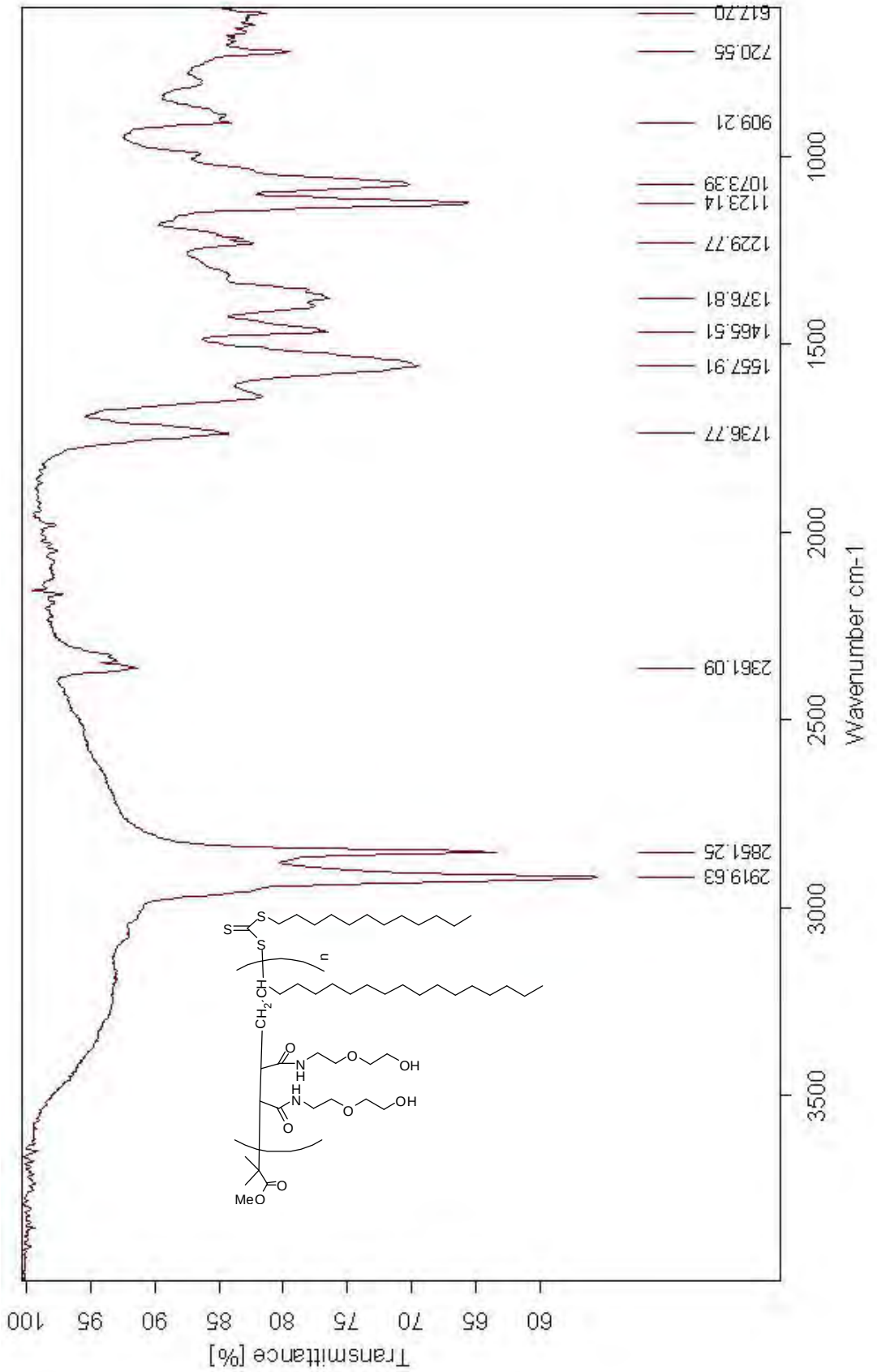

Figure 4.16 ATR-IR spectra of poly(maleic anhydride-*co*-1-octadecene) derivative

Table 4.12 ATR-IR absorption band assignment of poly(maleic anhydride-*co*-1-octadecene) derivative

Wave number (cm^{-1})	Intensity	Vibration
2920, 2851	Medium, medium	C-H stretching vibration of aliphatic hydrocarbon
1736	medium	C=O stretching vibration of amide
1169	Medium	C-N stretching vibration
1056	Medium	C-O stretching vibration

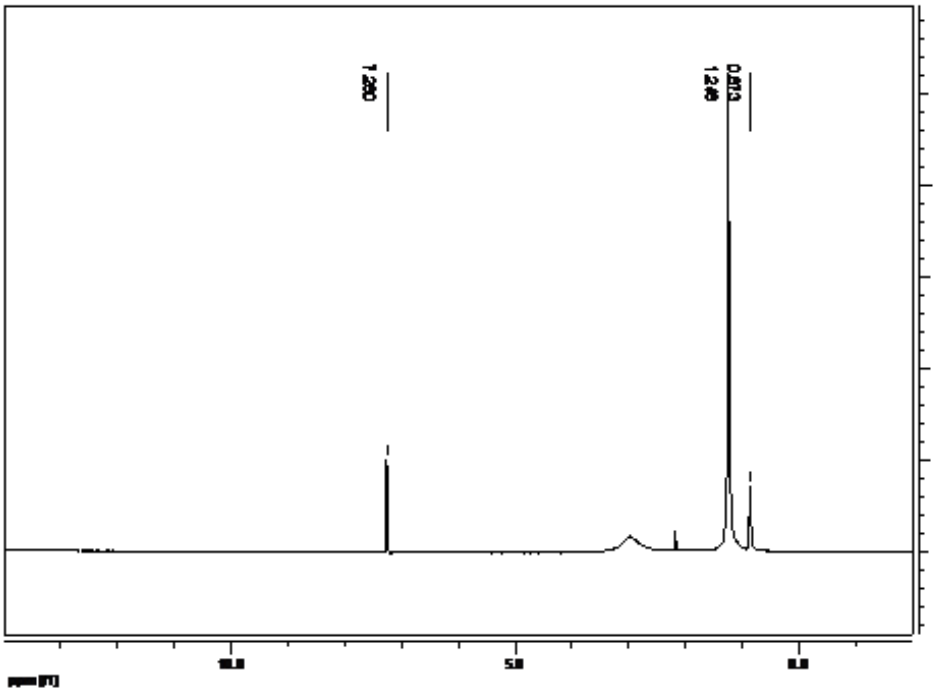

Figure 4.17 ^{1}H-NMR spectrum of poly(maleic anhydride-*co*-1-octadecene) derivative

Table 4.13 ^{1}H-NMR data assignment of poly(maleic anhydride-*co*-1-octadecene) derivative

Chemical Shift (ppm)	multiplicity	Details
0.8	multiplet	-$CH_2C\underline{H}_3$
1.2	multiplet	-$C\underline{H}_2$-
3.1	broad	-$OC\underline{H}_2CH_2$-

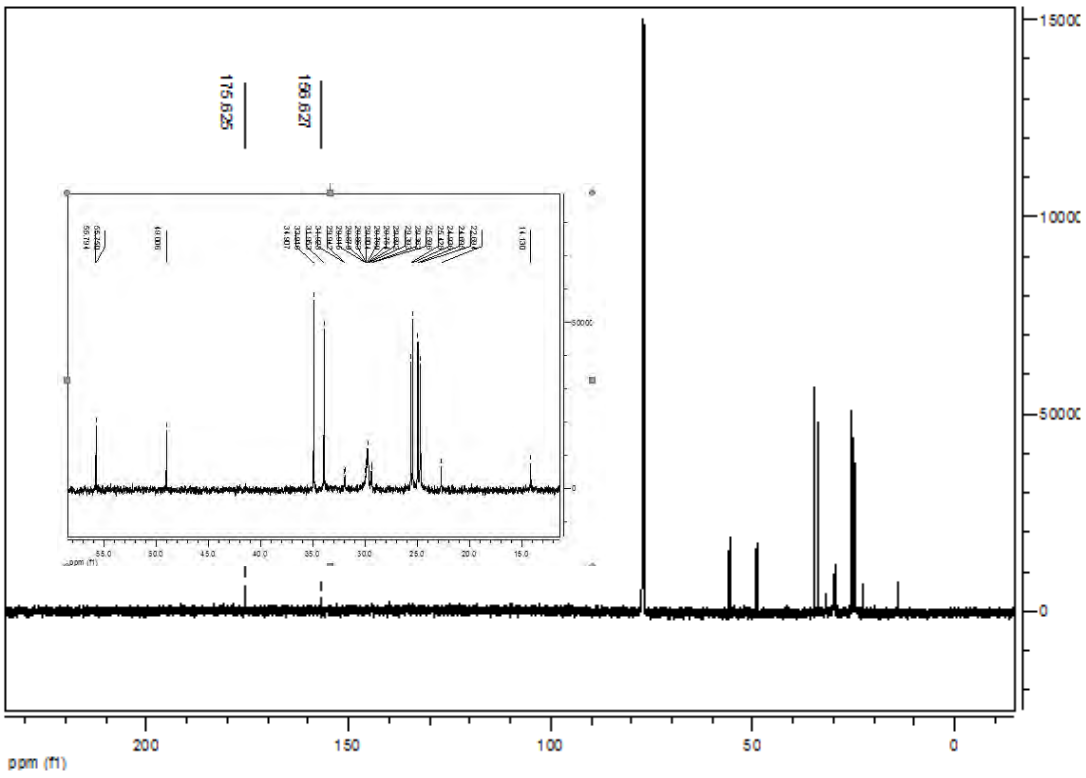

Figure 4.18 ^{13}C-NMR of poly(maleic anhydride-*co*-1-octadecene) derivative

Table 4.14 ^{13}C-NMR data assignment of poly(maleic anhydride-*co*-1-octadecene)-derivative

Chemical Shift (ppm)	Details
14.1	C-$\underline{C}H_3$
22.7,24.7, 24.9, 25.4, 25.6, 29.3, 29.4, 29.7 29.8, 29.8, 29.8, 29.9, 29.9, 30.0, 30.0,31.0 31.9, 33.9, 34.9	C-$\underline{C}H_X$-C
49.0, 55.8, 55.8	-$\underline{C}H_2$-O
156.6	-$\underline{C}$=S
175.6	-$\underline{C}$=O

4.3 Synthesis of monodispersed magnetite nanoparticles

Magnetite nanoparticles produced from the thermal decomposition of organometallics are extremely uniform in size, cryatallinity and shape. Because the formation of magnetite nanoparticles could be produced *via* the precursor iron carboxylate, this synthetic system relies on an iron carboxylate salt and 1-octadecene. The simple iron sources, FeO(OH) and oleic acid was reacted at high temperatures to produce the iron carboxylate precursors [54]. Interstingly, this iron source could completely dissolved in oleic acid at high temperature.

The amount of oleic acid was varied to study the effect of ligand to nanoparticles production as shown in Table 4.15. The result was investigated as the size of synthesized magnetite nanoparticles by TEM. The morphology of sample was investigated by a transmission electron microscope (TEM, JOEL 2010F, Tokyo, Japan). In addition, TEM samples were prepared by placing a drop test nanoparticle suspensions onto 300 mesh copper grid coated with carbon.

Table 4.15 Formula and result of magnetite nanoparticles production

Chemical	Condition		
	1	2	3
1) FeO(OH) (mmol)	10	10	10
2) Oleic acid (mmol)	40	60	80
3) Size[a] (nm)	11	18	32

a: the average size was measuring by TEM

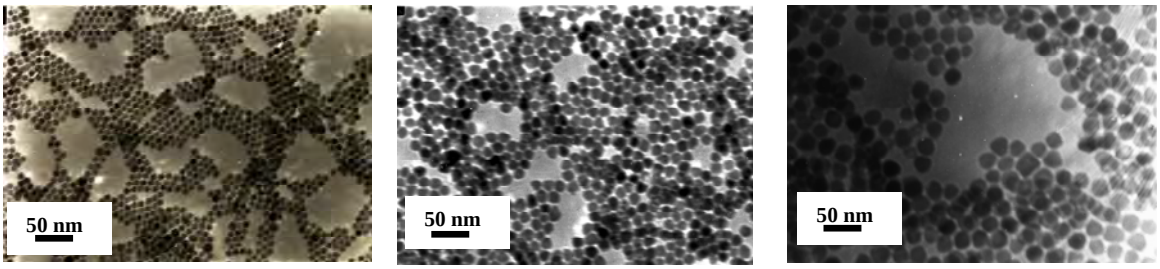

Figure 4.19 TEM image of the synthesized magnetite nanoparticles: made from condition 1 (left), condition 2 (middle), condition 3 (right)

According to the result in Table 4.15 and Figure 4.19, it was found out that when the amount of oleic acid was increase, the particles size of magnetite nanoparticles is directly proportional to the concentration of ligands. This could be explained that the higher ligand concentration, the lower the monomer reactivity was. Besides, there would be less nuclei was rapidly formed at the first stage, then the larger particle size was developed due to the availability of precursor in the solution phase. It was noted that magnetite nanoparticles prepared by this method was very stable in chloroform and no aggregation or precipitation was obvious over several months.

The X-ray diffraction determination of the magnetite nanoparticles, prepared by this method [54] was showed in Fig. 4.20. Six characteristic intensive diffractions of magnetite were appeared: Fe_3O_4 (2 2 0), Fe_3O_4 (3 1 1), Fe_3O_4 (4 0 0), Fe_3O_4 (4 2 2), Fe_3O_4 (5 1 1) and Fe_3O_4 (4 4 0) in the agreement with the literature [55].

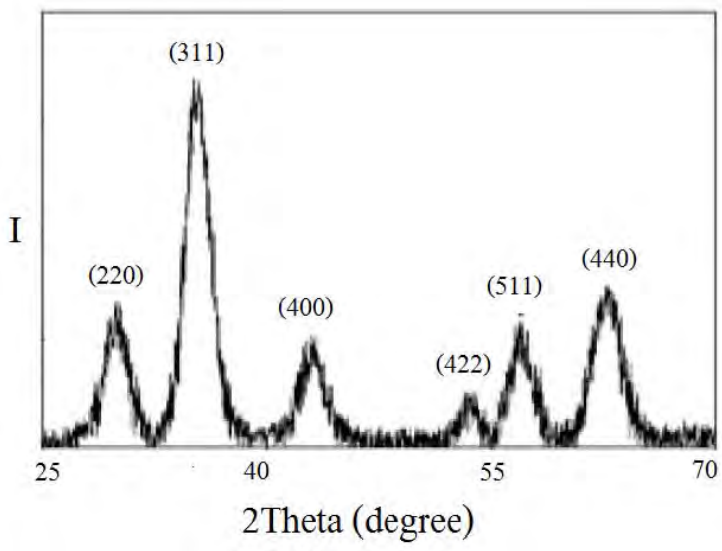

Figure 4.20 XRD patterns of the magnetite nanoparticles

4.4 Preparation of amphiphilic polymer-coated magnetite dispersion

As the matter of facts, magnetite is the most widely accepted nanoparticles material for biological application, as it is approved for use by the Food and Drug Administration in the application such as MRI contrast enhancement. However, magnetite nanoparticles are not dispersible in aqueous solution and their surface must first be modified prior to use in biomedical application. Many researchers have been focused on the improving dispersed ability of magnetite in water by using several compounds such as ligands, amphiphilic polymers as phase transfer agent. Among of these, there was a few report that was studied on the use of RAFT polymer for modified surface of magnetite. There are two main reasons on advantages of the use of RAFT techniques. Firstly, it has been reported previously the synthesized polymer was shown narrow molecular weight distribution. Secondly, the corresponding selected RAFT agents and initiator would generate telechelic amphiphilic polymer owning carboxylic group at one end and a thiol group at other end for further modification in biomedical application. From this point, the use of amphiphilic

polymer, synthesized by RAFT polymerization, for coating magnetite nanopaticles is highly interesting and challenging.

The simplified method based on forming micelles through amphiphilic polymers for transferring magnetite nanoparticles from organic solvents into water was used for the study. Regarding to this technique, the magnetite nanoparticles, which was originally dispersed in chloroform, could be completely transferred into water without any loss. The whole process was very simple and inexpensive. It also reduced the multi-step solution (buffer) exchange and purification, etc.

The synthesize monodisperse magnetite nanoparticles, 11 nm in diameter, was used as the reference model for polymer coating. The synthesized magnetite nanoparticles solution and the synthesized amphiphilic polymers were mixed in chloroform and kept stirring overnight at room temperature (the molar ratio of magnetite to amphiphilic polymer was 1 to 30). After that, the same volume of water was added; chloroform was then slowly removed by rotary evaporation at room temperature. The magnetite nanoparticles originally dispersed in chloroform were re-dispersed in water during the slow evaporation of chloroform. If the resulting solution was appeared as clear brown to dark solution, it could be expressed as the success of transferring magnetite nanoparticles to aqueous media.

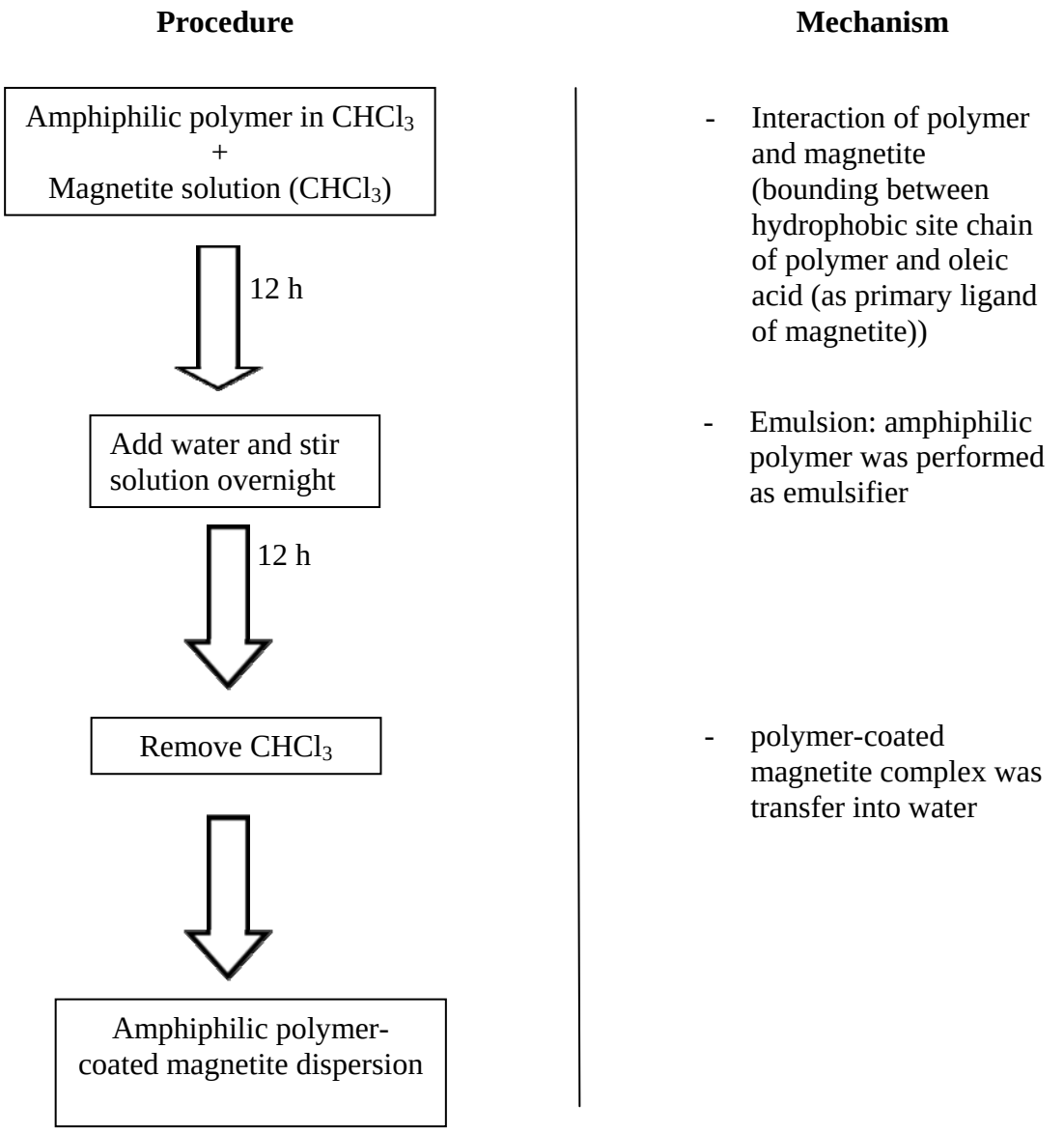

Scheme 4.6 Procedure for preparation of amphiphilic polymer-coated magnetite dispersion and mechanism

4.4.1 Preparation of poly(N-(2-hydroxyethyl)maleimide-*co*-1-octadecene)-coated magnetite dispersion

Poly(N-(2-hydroxyethyl)maleimide-*co*-1-octadecene) and the synthesized monodisperse magnetite nanoparticles, 11 nm in diameter, was mixed in chloroform. The resulting solution was observed as homogenous dark black solution because both poly(N-(2-hydroxyethyl)maleimide-*co*-1-octadecene) and the synthesize monodisperse magnetite nanoparticles were both excellent dissolved in chloroform. After adding of water, a cloud solution was appeared which was expected that the bounding of amphiphilic polymer and magnetite nanoparticle. After the evaporation of chloroform, the dark precipitate on the resulting solution was observed at the bottom of the reaction vessel as shown in Figure 4.21. This result was indicated the unsuccessful preparation of poly(N-(2-hydroxyethyl)maleimide-*co*-1-octadecene)-coated magnetite nanoparticles. This might be caused by the incomplete coating of a too short chain of the copolymer to the magnetite nanoparticles, leading particle could not be suspended well and then precipitated in water.

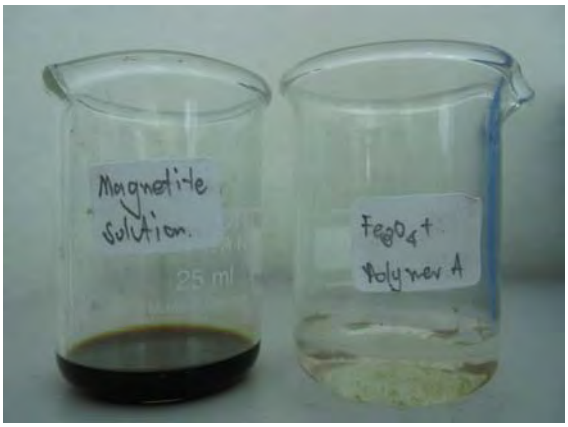

Figure 4.21 Pictures of magnetite nanopartcles in $CHCl_3$ (left) and a failure preparation of poly(N-(2-hydroxyethyl)maleimide-*co*-1-octadecene)-coated magnetite dispersion in water (right)

4.4.2 Preparation of poly(maleic anhydride-*co*-1-octadecene) derivative-coated magnetite dispersion

In order to prepare the poly(maleic anhydride-*co*-1-octadecene) derivative and the synthesize monodisperse magnetite nanoparticles, 11 nm in diameter, was mixed in chloroform. The resulting solution was observed as homogenous dark black solution because poly(maleic anhydride-*co*-1-octadecene) derivative and the synthesize monodisperse magnetite nanoparticles were both soluble in chloroform. After adding water to the resulting solution, clouding solution was observed. This was expected as the process of bounding between amphiphilic polymer and magnetite nanoparticles. After the slow evaporation of chloroform, the magnetite particles originally dispersed in chloroform were redispersed into water phase. As for Figure 4.22 poly(maleic anhydride-, it showed the success of preparation of poly(maleic anhydride-*co*-1-octadecene) derivative -coated magnetite dispersion in water as the clear brown solution compared to the originated magnetite nanopartcles in $CHCl_3$.

Figure 4.22 Pictures of magnetite nanopartcles in $CHCl_3$ (left) and poly(maleic anhydride-*co*-1-octadecene) derivative -coated magnetite dispersion in water (right)

With regard to the study of the morphology of the preparative poly(maleic anhydride-*co*-1-octadecene) derivative -coated magnetite dispersion by TEM, the sample of poly(maleic anhydride-*co*-1-octadecene)derivative-coated magnetite dispersion need to be purified more. The resulting sample solution was passed through a 0.2 µm nylon syringe filter. Then, an ultracentrifuge was used to remove excess amphiphilic polymer at 300000 g for 2 h. The sample was re-dispersed into water and taken to determine its morphology by TEM.

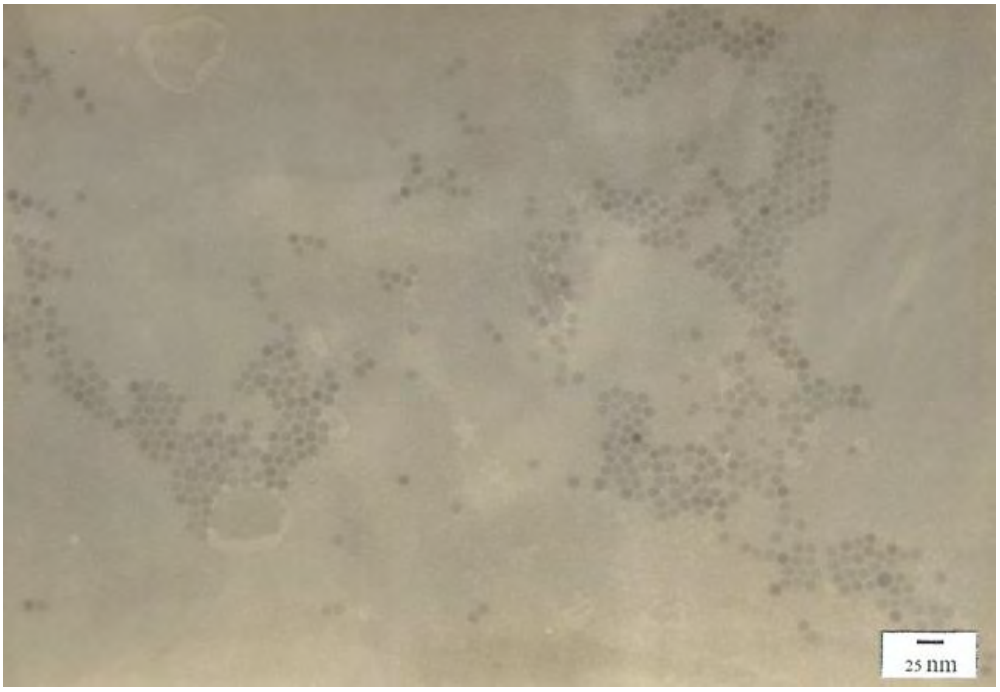

Figure 4.23 TEM image of poly(maleic anhydride-*co*-1-octadecene) derivative -coated magnetite dispersion

In Figure 4.23, the average particle size of poly(maleic anhydride-*co*-1-octadecene) derivative -coated magnetite dispersion was measured as 13 nm by TEM. The complex was investigated as small and size uniformed magnetite complex nanoparticles

4.4.3 Proposed model of poly(maleic anhydride-*co*-1-octadecene) derivative -coated magnetite dispersion

The proposed model structure of the complex of poly(maleic anhydride-*co*-1-octadecene) derivative -coated magnetite dispersion was shown in Figure 4.24. Oleic acid was coated over magnetite nanoparitcles as primary layer, by using its carboxylic acid functional group bounded to the surface of magnetite and turned its long chain hydrocarbon positioned as the outer part. Then, the hydrophobic site of amphiphilic polymer will be bounded to the hydrocarbon chain of oleic acid, generating the second layer of the complex. The hydrophilic ethylene glycol units and end terminal carboxylic acid of copolymer was bonded to neighboring waters to make the nanoparticles complex could be dispersed in water media.

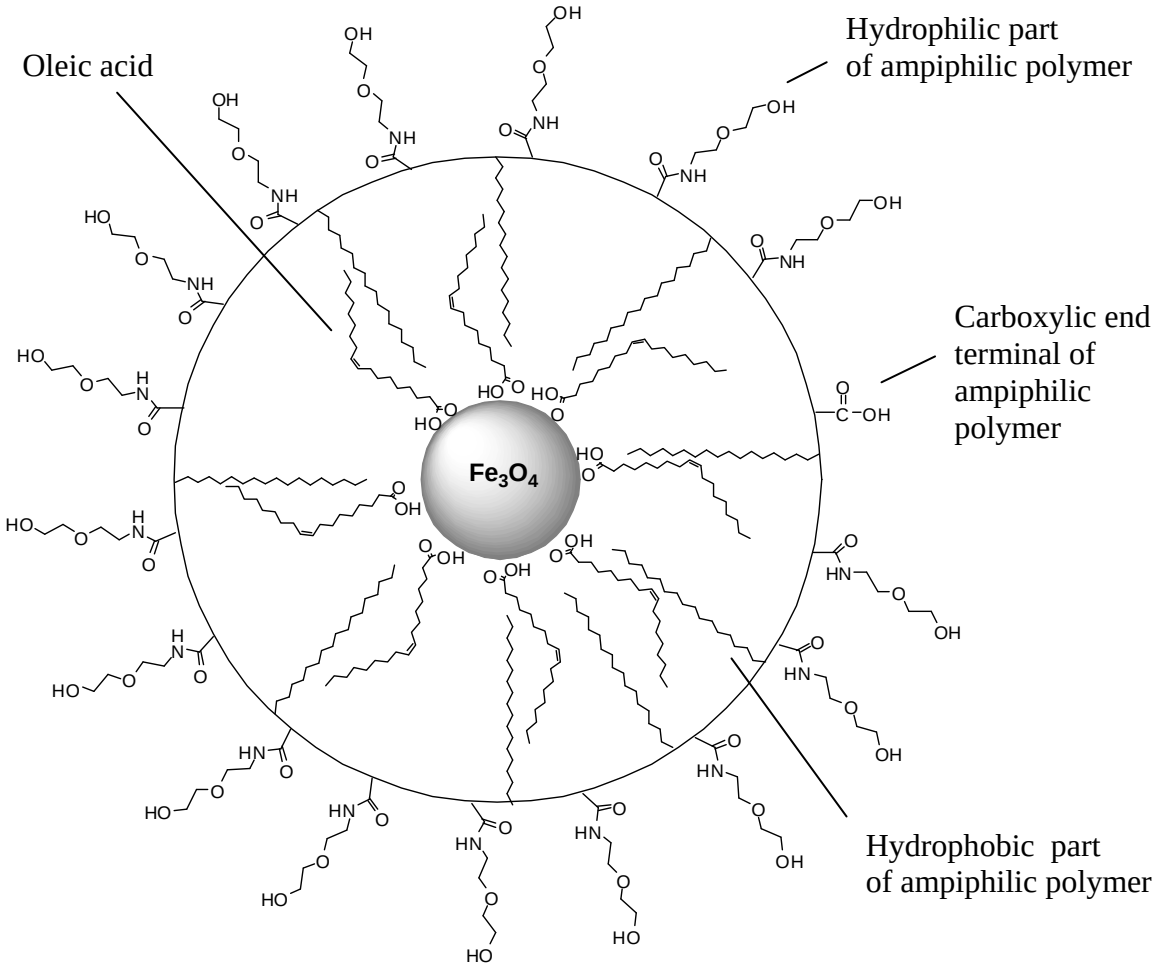

Figure 4.24 The proposed model of poly(maleic anhydride-*co*-1-octadecene) derivative-coated magnetite dispersion

CHAPTER V

CONCLUSIONS AND SUGGESTIONS

The main feature of this research is to search for new kind of amphiphilic polymer which was typical as hydrophobic hydrocarbon and hydrophilic ethylene glycol type. These novel amphiphilic polymers were used for the preparation of the magnetite complexion dispersion.

According to this research study, two kind of copolymers, poly (N-(2-hydroxyethyl)maleimide-*co*-1-octadecene) and poly(maleic anhydride-*co*-1-octadecene) were successfully accomplished by RAFT technique.

As for the synthesis of poly (N-(2-hydroxyethyl)maleimide-*co*-1-octadecene), there was no significant different on Mn and Mw of copolymer when various reaction temperature, 70-90^{o}C and type of solvent, THF and 1,4-dioxane was employed for the study. For polymerization at 70^{o}C in THF, the highest Mn and Mw of poly (N-(2-hydroxyethyl)maleimide-*co*-1-octadecene) was observed by GPC as 1026 and 1453 D, respectively.

In accordance with the synthesis of poly(maleic anhydride-*co*-1-octadecene), the copolymer was obtained as 11870 D of Mn and 21047 D of Mw after polymerization at 90 ^{o}C in 1,4-dioxane for 12 h. Amphiphilic poly(maleic anhydride-*co*-1-octadecene) derivative was successfully prepared by ring opening of poly(maleic anhydride-*co*-1-octadecene) utilizing 2-(2-aminoethoxy)-ethanol and coupling reaction for amide formation. poly(maleic anhydride-*co*-1-octadecene) derivative was conformed the construction of the compound by ATR-IR, ^{1}H-MNR and ^{13}C-NMR.

Monodispersed magnetite nanoparticles was produced by thermal decomposition of FeO(OH) utilizing oleic acid as primary ligand. The smallest size of magnetite nanoparticles was prepared and obtained as 11 nm in diameter by TEM.

Amphiphilic polymer-coated magnetite dispersion was successfully prepared by using poly(maleic anhydride-*co*-1-octadecene) and synthesized magnetite nanoparticles solution. The TEM result was revealed the particle size of complex as 13 nm in diameter. A preparation of the complex of poly (N-(2-hydroxyethyl)maleimide-*co*-1-octadecene) and magnetite nanoparticles solution was not successful because of an incompleted coating of short molecular weight polymer to magnetite.

5.1 Further works

1. To study the magnetic properties of the prepared magnetite nanoparticles and amphiphilic polymer-coated magnetite dispersion.

2. To modified amphiphilic polymer-coated magnetite dispersion for biomedical application.

REFERENCES

[1] Lalatonne, Y., Richardi, J. and Pileni, M.P. Van der Waals versus dipolar forces controlling mesoscopic organizations of magnetic nanocrystals. Nat. Mater. 3 (2004): 121-125.

[2] Tang, D.S., and others. Preparation of monodispersed multi-walled carbon nanotubes in chemical vapor deposition. Chem. Phys. Lett. 356 **(**2002): 563-566.

[3] Moser, A., and others. Magnetic recording: advancing into the future. J. Phys. D: Appl. Phys. 35 (2002): 157-167.

[4] Matsushita, N., Chong, C.P., Mizutani, T. and Abe, M. Ni–Zn ferrite films with high permeability (μ' = ~30, μ'' = ~30) at 1 GHz prepared at 90 °C. J. Appl. Phys. 91 (2002): 7376-7378.

[5] Sorenson, T.A., Morton, S.A., Waddill, G.D., and Switzer, J.A. Epitaxial electrodeposition of Fe_3O_4 thin films on the low-index planes of gold. J. Am. Chem. Soc. 124 (2002): 7604-7609.

[6] Yean, S., and others. Effect of magnetite particle size on adsorption and desorption of arsenite and arsenate. J. Mater. Res. 20 (2005): 3255-3264.

[7] Song, H.-T., and others. Surface modulation of magnetic nanocrystals in the development of highly efficient magnetic resonance probes for intracellular labeling. J. Am. Chem. Soc. 127 (2005): 9992-9993.

[8] Nam, J.-M., Thaxton, C.S., and Mirkin, C. A. Nanoparticle-based bio-bar codes for the ultrasensitive detection of proteins. Science 301 (2003): 1884-1886.

[9] Shinkai, M., and Ito, A. Functional magnetic particles for medical application. Adv. Biochem. Eng. Biotechnol. 91 (2004): 191-220.

[10] Gupta, A.K., and Gupta, M. Synthesis and surface engineering of iron oxide nanoparticles for biomedical applications. Biomaterials 26 (2005): 3995-4021.

[11] Horak, D., Rittich, B., and Spanova, A. Carboxyl-functionalized magnetic microparticle carrier for isolation and identification of DNA in dairy products. J. Magn. Magn. Mater. 311 (2007): 249–254.

[12] Chin, A.B. and Yaacob, I.I. Synthesis and characterization of magnetic iron oxide nanoparticles via w/o microemulsion and Massart's procedure. J. Mater. Process. Technol. 191 (2007): 235–237.

[13] Albornoz, C. and Jacobo, S.E. Preparation of a biocompatible magnetic film from an aqueous ferrofluid. J. Magn. Magn. Mater. 305 (2006): 12-15.

[14] Kim, E.H., Lee, H.S. Kwak, B.K., and Kim, B.K. Synthesis of ferrofluid with magnetic nanoparticles by sonochemical method for MRI contrast agent. J. Magn. Magn. Mater. 289 (2005): 328-330.

[15] Kimata, M., Nakagawa, D., and Hasegawa, M. Preparation of monodisperse magnetic particles by hydrolysis of iron alkoxide. Powder Technol. 132 (2003): 112-118.

[16] Jain T.K., Morales, M.A., Sahoo, S.K., Leslie-Pelecky, D.L. and Labhasetwar, V. Iron oxide nanoparticles for sustained delivery of anticancer agents. Mol. Pharmarcet. 2 (2005): 194-205.

[17] Lee, P.-W., and others. The characteristics, biodistribution, magnetic resonance imaging and biodegradability of superparamagnetic core–shell nanoparticles. Biomaterials 31 (2010): 1316-1324.

[18] Boyer, C., Bulmus, V., Davis, T.P., Ladmiral, V., Liu, J., and Perrier, S. Bioapplications of RAFT polymerization. Chem. Rev. 109 (2009): 5402-5436.

[19] Colombani, D. Chain-growth control in free radical polymerization. Prog. Polym. Sci. 22 (1997): 1649-1720.

[20] Percec, V. Introduction: frontiers in polymer chemistry. Chem. Rev. 101 (2001): 3579-3580.

[21] Jose, M.M.-M., Tomas, R.B., and Pedro, J.P. Efficient atom-transfer radical polymerization of methacrylates catalyzed by neutral copper complexes. Macromolecules 43 (2010): 3221–3227.

[22] Hawker, C.J., Bosman, A.W.; Harth, E. New polymer synthesis by nitroxide living radical polymerization. Chem. Rev. 101 (2001): 3661–3688.

[23] Chiefari, J., and others. Living free-radical polymerization by reversible addition−fragmentation chain transfer: The RAFT Process. Macromolecules 31 (1998): 5559-5562.

[24] Lowe, A.B. and McCormick, C.L. Reversible addition–fragmentation chain transfer (RAFT) radical polymerization and the synthesis of water-soluble (co)polymers under homogeneous conditions in organic and aqueous media. Prog. Polym. Sci. 32 (2007): 283–351.

[25] Chong, Y.K., Krstina, J., Le, T.P.T., Moad, G., Postma, A., Rizzardo, E., and Thang, S.H. Thiocarbonylthio compounds [SC(Ph)S-R] in free radical polymerization with reversible addition-fragmentation chain transfer (RAFT polymerization). Role of the free-radical leaving group (R). Macromolecules 36 (2003): 2256-2272.

[26] Chiefari, J., and others. Thiocarbonylthio compounds (SC(Z)S-R) in free radical polymerization with reversible addition-fragmentation chain transfer (RAFT polymerization). Effect of the activating group Z. Macromolecules 36 (2003): 2273-2283.

[27] Kim, D.H., and others. Surface-modified magnetite nanoparticles for hyperthermia: Preparation, characterization, and cytotoxicity studies. Curr. Appl. Phys. 6 (2006): 242–246.

[28] Bergemann, C., Muller-Schulte, D., Oster, J., Brassard, L. and Lubbe, A.S. Magnetic ion-exchange nano- and microparticles for medical biochemical and molecular biological applications. J. Magn. Magn. Mater. 194 (1999): 45-52.

[29] Jolivet, J.P., Chaneac, C., and Tronc, E. Iron oxide chemistry. From molecular clusters to extended solid networks Chem. Commun. 5 (2004): 481-487.

[30] Park, J. and others. Preparation of water-soluble magnetite nanocrystals from hydrated ferric salts in 2-pyrrolidone: mechanism leading to Fe_3O_4. Angew. Chem. Int. Ed. 44 (2005): 123-126.

[31] Duraes, L., Costa, B.F.O., Vasques, J., Campos, J., and Portugal, A. Phase investigation of as-prepared iron oxide/hydroxide produced by sol–gel synthesis. Mater. Lett. 59 (2005): 859-863.

[32] Xu, J. and others. Preparation and magnetic properties of magnetite nanoparticles by sol–gel method. J. Magn. Magn. Mater. 309 (2007): 307-311.

[33] Abu, M.-Q.R., and Gedanken, A. Sonochemical synthesis of stable hydrosol of Fe_3O_4 nanoparticles. J. Phys. Chem. B 284 (2005): 489-492.

[34] Amstad, E., Gillich, T., Bilecka, I., Textor, M., and Reimhult, E. Ultrastable iron oxide nanoparticle colloidal suspensions using dispersants with catechol-derived anchor groups. Nano Lett. 9 (2009): 4042-4048.

[35] Miles, W.C., and others. The design of well-defined PDMS–magnetite complexes. Polymer 51 (2010): 482-491.

[36] Cha, Y.-J., and others. Synthesis and characterizations of surface-coated superparamagnetic magnetite nanoparticles. IEEE Trans. Magn. 46 (2010): 443-446.

[37] Jain, T.K., Morales, M.A., Sahoo, S.K., Leslie-Pelecky, D.L., and Labhasetwar, V. Iron oxide nanoparticles for sustained delivery of anticancer agents. Mol. Pharmarcet. 2 (2005): 194-205.

[38] Lee, P.-W., and others. The characteristics, biodistribution, magnetic resonance imaging and biodegradability of superparamagnetic core–shell nanoparticles. Biomaterials 31 (2010): 1316-1324.

[39] Hong, R.Y., and others. Synthesis, characterization and MRI application of dextran-coated Fe_3O_4 magnetic nanoparticles. Biochem. Eng. J. 42 (2008): 290-300.

[40] Kim, D.K., Zhang, Y., Kehr, J., Klason, T., Bjelke, B., and Muhammed, M. Characterization and MRI study of surfactant-coated superparamagnetic nanoparticles administered into the rat brain" J. Magn. Magn. Mater. 225 (2001): 256-261.

[41] Shultz, M.D., Calvin, S., Fatouros, P.P., Morrison, S.A. and Carpenter, E.E. Enhanced ferrite nanoparticles as MRI contrast agents. J. Magn. Magn. Mater. 311 (2007): 464-468.

[42] Yang, S., Liu, H., Huang, H., and Zhang, Z. Fabrication of superparamagnetic magnetite/ poly(styrene-*co*-12-acryloxy-9-octadecenoic acid) nanocomposite microspheres with controllable structure. J. Colloid Interf. Sci. 338(2009): 584–590

[43] Podzus, P.E., Daraio, M.E., and Jacobo, S.E. Chitosan magnetic microspheres for technological applications: Preparation and characterization. Physica B 404 (2009): 2710–2712.

[44] Moolekamp, F.E., and Stokes, K.L. Magnetooptical Response of Gold-Magnetite Nanocomposite Films. IEEE Trans. Magn. 45 (2009): 4888-4891.

[45] Abdalla, M.O., and others. Synthesis and characterization of noscapine loaded magnetic polymeric nanoparticles. J. Magn. Magn. Mater. 332 (2010): 190–196.

[46] Yang, C., Shao, Q., He, J., and Jiang, B. Preparation of monodisperse magnetic polymer microspheres by swelling and thermolysis technique. Langmuir 26 (2010): 5179-5183.

[47] Basavaraja, C., Jo, E.A., and Huh, D.S. Characterization and magnetic properties of conducting poly(N-vinylcarbazole)-capped magnetite nanocomposite Langmuir-Schaefer film. Mat. Lett. 64 (2010): 762-764.

[48] Kavas, H., Durmus, Z., Baykal, A., Aslan, A., Bozkurt, A., and Toprak, M.S. Synthesis and conductivity evaluation of PVTri-Fe_3O_4 nanocomposite. J. Non-Cryst. Solids 356 (2010): 484–489

[49] Frickel, N., Messing, R., Gelbrich, T., and Schmidt, A.M. Functional silanes as surface modifying primers for the preparation of highly stable and well-defined magnetic polymer hybrids. Langmuir 26 (2010): 2839-2846.

[50] Bhatt,A.S., Bhat, D.K., and Santosh, M.S. Electrical and magnetic properties of chitosan-magnetite nanocomposites. Physica B 405 (2010): 2078–2082

[51] Hsiao, S.-C., Ou, J.-L., Sung, Y., Chang, C.-P., and Ger, M.-D. Preparation of sulfate- and carboxyl-functionalized magnetite/polystyrene spheres for further deposition of gold nanoparticles. Colloid Polym. Sci. 288 (2010): 787–794.

[52] Lai, T.J., Filla, D., and Shea, R. Functional polymers from novel carboxyl-terminated trithiocarbonates as highly efficient RAFT agents. Macromolecules 35 (2002): 6754-6756.

[53] Ma, J., Cheng, C., Sun, G., and Wooley, K.L. Well-defined polymers bearing pendent alkene functionalities via selective RAFT polymerization. Macromolecules 41 (2008): 9080-9089.

[54] Yu, W.W., Falkner, J.C., Yavuz, C.T., and Colvin, V.L. Synthesis of monodisperse iron oxide nanocrystals by thermal decomposition of iron carboxylate salts. Chem. Commun. 20 (2004): 2306-2307.

[55] Janakya, C., Endrodi, B., Kovacs, K., Timkoc, M., Sapid, A., and Visya, C. Chemical synthesis of poly(3-thiophene-acetic-acid)/magnetite nanocomposites with tunable magnetic behavior. Synthetic Met. 160 (2010): 65-71.

VITAE

Ong-art Thanetnit received his Master degree of Science in Chemistry from Chulalongkorn University in 2005. After graduating, he studied in Ph.D. program in Chemistry from Chulalongkorn and joined Assoc. Prof. Supawan's Laboratory since 2007. He was awarded Graduate Studies Education Support Scholarship on the Occasion of His Majesty the King's 72nd Birthday from Chulalongkorn University during 2005-2008, Professor Tab Foundation Scholarship in 2008 and was also supported a research grant for his Ph.D. dissertation by Graduate School of Chulalongkorn University. During his doing research abroad, he joined Assoc. Prof. William W. Yu's Nano-Laboratory in 2008 and was awarded as a teaching assistantship by Chemistry and Biochemistry program from Worcester Polytechnic Institute (WPI), USA, in 2008-2009.